2012

Technoeconomic analysis of biorefinery based on multistep kinetics and integration of geothermal energy

Sudhanya Banerjee
Iowa State University

Technoeconomic analysis of biorefinery based on multistep kinetics and integration of geothermal energy

by

Sudhanya Banerjee

A thesis submitted to the graduate faculty

in partial fulfillment of the requirements for the degree of

MASTER OF SCIENCE

Major: Mechanical Engineering

Program of Study Committee:
Song-Charng Kong, Major Professor
Robert C. Brown
Guiping Hu

Iowa State University

Ames, Iowa

2012

TABLE OF CONTENTS

LIST OF FIGURES

LIST OF TABLES

ACKNOWLEDGEMENT

First of all, I would express my gratitude towards my major professor Dr. Song-Charng Kong for offering me the opportunity to work on the project which potentially aims towards offering an alternative solution to the surmounting energy crisis and increasing greenhouse gas emissions. Dr. Kong's commitment is worth mentioning throughout my work whenever I needed him in times of confusion and difficulties.

I would also like to express my gratitude to Dr. Robert C. Brown and Dr. Guiping Hu for devoting their valuable time to serve as my committee members. Their feedback has been significantly important for making my work better.

A great deal of assistance has been provided to me by the staff in the Department of Mechanical Engineering. I thank Amy Carver, Nate Jensen, Deb Schroeder and Carol Knutson for their administrative and technical support throughout this project.

I would like to thank Tristan Brown and the entire Technoeconomic analysis research group for valuable inputs in the work. My fellow graduate students and group members have provided valuable help and discussion throughout this program. I would like to thank the members of Dr. Kong's research group for making this work enjoyable and for providing guidance and support along the way. In particular, I thank Jordan Alan Tiarks, Sujith Sukumaran, Cuong Van Huynh, and Yanan Zhang for all you have done.

Finally, I would like to thank my family and friends for all of their support. To my parents – The sacrifices you have made and the love and encouragement you have given to me have provided a world of possibilities and have helped me become the person I am today. From the bottom of my heart, thank you for all you have done.

ABSTRACT

In this work, a technoeconomic study is conducted to assess the feasibility of integrating geothermal energy into a biorefinery for biofuel production. The biorefinery is based on a thermochemical conversion platform that converts 2,000 metric tons of corn stover per day into biofuels via gasification. Geothermal heat is utilized in the biorefinery to generate process steam for gasification and steam-methane reforming. A process simulation model is developed to simulate the operation of the proposed biorefinery, and corresponding economic analysis tools are utilized to predict the product value. Process steam at 150 ºC with a flow rate of approximately 16 kg/s is assumed to be generated by utilizing the heat from geothermal resources producing a geothermal liquid at 180 °C and a total flowrate of 105 kg/s. In addition to the use for gasification and steam-methane reforming, additional geothermal capacity at 100 kg/sec from multiple wells is used for electricity production via Organic Rankine Cycle to add to the profitability of the biorefinery. The total capital investment, operating costs, and total product values are calculated considering an operating duration of 20 years for the plant and the data are reported based on the 2012 cost year. Simulation results show that the price of the fuel obtained from the present biorefinery utilizing geothermal energy ranges from $5.18 to $5.50 per gallon gasoline equivalent, which is comparable to $5.14 using the purchased steam. One important incentive for using geothermal energy in the present scenario is the reduction of greenhouse gas emissions resulting from the combustion of fossil fuels used to generate the purchased steam. Geothermal energy is an important renewable energy resource, and this study provides a unique way of integrating geothermal energy into a biorefinery to produce biofuels in an environmentally friendly manner.

In the other part of the study, the simulation of biomass gasification is carried out using multistep kinetics under various oxygen-enriched air and steam conditions. The oxygen percentage is increased from 21% to 45% (by volume). Five different kinds of biomass feedstocks including pine wood, maple-oak mixture (50/50 by weight), seed corn, corn stover, and switchgrass are used in this study. The bed temperature is maintained at 800 ^{o}C. Different conditions such as flowrates of biomass and different oxygen-enriched air and steam ratios are used to simulate different cases. The simulation results for different species are in good agreement with the experimental data.. From the results, it is evident that the proposed gasification kinetics model can predict the syngas compositions. The model is able to capture the effects of biomass feedstock and oxygen and steam concentrations. The model is able to predict the concentrations of H_2, CO, CO_2, H_2O, CH_4, N_2 in the syngas; nonetheless, more rigorous simulation has to be carried out to model NO_x, NH_3, and other higher alkane and alkenes such as C_2H_4, C_2H_2, C_2H_6 etc.

CHAPTER 1. INTRODUCTION

1.1 Motivation

Energy has always been the foundation for growth in population, economy and technologies. Worldwide, fast growing population coupled with evermore energy dependent technologies in the modern age indicates that energy demands are expected to rise dramatically. Fossils fuels—natural gas, petroleum, and coal—has made up the majority of the world's energy supply; however, fossil fuel reserves are finite and fast depleting. Also, the usage in fossil fuels has led to the increased emissions that are harmful to human health and environment. In order to avoid these hazards, the use of renewable energy such as hydropower, geothermal, wind, solar, and biomass has been gaining significant interest. The use of renewable energy has additional advantages besides mitigating the life-cycle greenhouse (GHG) emissions and petroleum fuel shortage. For example, the development and use of renewable energy can help many countries stabilize national energy supply and become less dependent on foreign oils. Furthermore, renewable energy can enhance the economic development of rural areas.

According to the Energy Information Administration (EIA), the renewable energy sector is projected to be the fastest growing sector of energy supply for the years from 2009 to 2035. In this sector, total biomass energy is projected to grow at a rate of 2.9% per year with specific areas growing at even higher rates including electricity generation growing by up to 5.6% per year (EIA 2011). This rapid growth can be attributed to a variety of causes including new policy decisions that have shaped the future energy market, economic uncertainty in the last decade, and growing environmental concerns due to GHG emissions. In 2009, the EPA issued a revised Renewable Fuel Standard (RFS2) that set increased

minimum biorenewable transportation fuel mandates through the year 2022. Additionally, in order to qualify as a renewable fuel, life cycle analysis of each type of fuel must confirm that the renewable fuel produces a net reduction in GHG emissions, with different benchmarks for the type of fuel and the amount of GHG reduction (EPA 2010). This policy means that methods of energy generation now play a significant role in the net benefit from a given biofuel, and some ethanol refineries that gain electricity and process heat from coal would no longer qualify as a renewable fuel. Finally, the EPA has proposed a new carbon pollution standard (expected to become a policy) for all future new power plants that calls for a 50% reduction in carbon emissions from coal fired power plants (Tiarks 2012). This effectively limits new power plants to be based on natural gas or other clean energy sources such as biomass (EPA 2012).

1.2 Biomass and Geothermal Energy

Biomass, defined as any organic materials of recent biological origin (Brown, 2003), includes agricultural crop residues, forest residues, energy crops, organic municipal wastes (MSW), and animal wastes. Biomass has been the earliest energy resource gathered and utilized by humankind. Upon the discovery of fossil fuels during 19th and 20th centuries, the use of biomass as energy sources have been drastically declined (Biomass Technology Group, 2005). However, there has been a recent renewed interest in using biomass as energy sources driven by increased global energy demands, coupled with diminishing fossil fuel supplies.

Biomass is an attractive energy resource with 12 billion tons (equivalent to 270 EJ of energy content) available worldwide annually on sustainable basis (Tester, Drake et al. 2005).

Unlike, fossil fuels, biomass is sustainable and is the only renewable hydrocarbon resource that can fulfill the dual roles of substitution for fossil fuels and help mitigate global climate challenges. The use of these biomass products for chemical, heat and power, and transportation fuels has low net carbon release to the atmosphere. This is because the fixed carbon in biomass when burned will be consumed as new biomass are planted and grow, thus their use does not add to the overall atmospheric carbon. However, fuel and energy production from biomass require energy inputs from fossil fuels during agricultural production and operation of equipment in the production plants thus resulting in non-zero net carbon cycle.

Biochemical conversion technologies is a relatively mature technology and is widely used in biofuel production (Basu 2010). However, it may not be the most effective method in utilizing biomass resources, depending on the feedstock. Production of biofuels (ethanol and biodiesel) from fermentation or catalytic processes is only possible with food crops (corn, sugarcane, wheat, barley, sorghum, etc.) as the feedstock. Consequently, this leads to the controversy of "Food vs. Fuel" debates as well as the possible surges in the food prices. Besides, fermentation is only feasible with large developed countries such as the U.S. where agricultural production exceeds the required food and animal feed needs. Thus there is an urgent need for technologies that can operate on non-edible biomass (wood, switchgrass, energy crops, MSW, and animal wastes) for production of biofuels with high efficiency.

Thermochemical conversion of biomass is a promising technology that can exploit the embedded energy within various kinds of biomass and convert into valuable intermediates with flexibility for many industrial market applications such as heat, electricity

and liquid fuels (Chen et al., 2007). Biomass gasification is one of the technologies currently being investigated which could show great promises in meeting the environmental, economic, and policy concerns of the current decade and into the future. Biomass gasification is a thermo-chemical process that generates producer gas or synthesis gas when the biomass feedstock is exposed to a high temperature, fuel rich environment in the presence of air, steam, and/or oxygen as a fluidizing agent(Li, Grace et al. 2004). Gasification is the partial oxidation of solid, carbonaceous fuels into low energy content flammable gas mixtures consisting of carbon monoxide (CO), hydrogen (H_2), nitrogen (N_2), carbon dioxide (CO_2), and a variety of hydrocarbons utilizing high temperatures between 500 to 1400 °C and some mixture of air, oxygen and/or steam as a fluidizing agent. Gasification is a rather old concept that was commercialized as early as 1812 when coal was converted to "town gas" for use in lighting the streets at night. This technology was spread throughout the industrialized world until a ready supply of natural gas became a cheap alternative in the 1950s. In addition to its history of providing town illumination, gasification has been used as a source of direct fuel and fuel stock during times of energy shortages. During World War II, many people converted their automobiles to run using wood-derived town gas. In times of fuel shortages due to war or embargo, gasification has also served to provide a fuel feedstock for Fischer-Tropsch synthesis of liquid transportation fuels (Brown 2003).

In addition to biomass, geothermal energy is also an important source of renewable energy. Resources of geothermal energy range from the shallow ground to hot water and hot rock found a few miles beneath the Earth's surface, and down even deeper to the extremely high temperature of molten rock called magma. Currently, United States of America has the

greatest potential for geothermal energy production (Tester, Drake et al. 2005). The energy content of domestic geothermal resources to a depth of 3 km (~2 mile) is estimated to be 3 million quads (Bruce D. Green 2006). Geothermal power plants emit little carbon dioxide, very low quantities of sulfur dioxide, and no nitrogen oxides. U.S. geothermal generation annually offsets the emission of 22 million metric tons of carbon dioxide, 200,000 tons of nitrogen oxides, and 110,000 tons of particulate matter from conventional coal-fired plants (Bruce D. Green 2006). Geothermal energy can be utilized for direct heating, heat pumps, and for electricity production.

1.3 Objective

The objective of this study is to investigate the economic feasibility of the thermochemical pathway of gasification to produce transportation fuels and the integration potential of geothermal energy into the gasification-based biorefinery. First, this study will study the feasibility of producing liquid transportation fuels with electricity as a byproduct via biomass gasification using the available technology within the next decade. Second, methods of utilizing geothermal energy in a biorefinery and the corresponding economic impacts are discussed.

This study will compare capital investment costs and production costs for n^{th} plant biorefinery scenarios based on gasification. In this particular study, simulation of biomass gasification is carried out using a multi-step kinetics under various oxygen-enriched air and steam conditions. The oxygen percentage is increased from 21% to 45% (by volume). Experimental data from five different kinds of biomass feedstocks including pine wood, maple-oak mixture (50/50 by weight), seed corn, corn stover, and switchgrass are used for

model validation. On the other hand, in a regular biorefinery, heat and steam are generated by the combustion of fossil fuels and are required for various processes. By using geothermal energy in the biorefinery, the demand for fossil fuels is reduced, thus reducing overall greenhouse gas emissions. In addition, excess geothermal energy can be used for electricity generation using Organic Rankine Cycle (ORC). Such integration provides a new way of combining two renewable energy technologies to produce renewable fuels.

CHAPTER 2. LITERATURE REVIEW

2.1 Gasification Biorefinery

Biomass is a renewable energy source and has the potential to supply a large amount of energy with less environmental impact than fossil fuels. The use of biomass as an energy source has increased in recent years and has the advantage of reducing overall carbon emissions (Tester, Drake et al. 2005). Biomass can be converted to commercial products via biological or thermochemical processes (Caputo, Palumbo et al. 2005; Yoshioka, Hirata et al. 2005; Lin 2006). While mature technologies exist for biological conversion of biomass to transportation fuels (e.g., corn ethanol and soy biodiesel), the biological conversion of low-value lignocellulosic, non-food biomass still faces technological and economic challenges. On the other hand, combustion, pyrolysis and gasification are the three main thermochemical conversion methods that are of current interest in converting non-food biomass to heat, power, and/or fuels. Thermochemical gasification is a promising technology that can exploit the embedded energy within various types of biomass and convert into valuable intermediates with flexibility for many industrial market applications such as biofuels, valuable chemicals, and heat and power. Traditionally biomass is burned to supply heat and power in the process and power industries. The net efficiency for electricity generation from biomass combustion ranges from 20% to 40% (Caputo, Palumbo et al. 2005). Pyrolysis converts biomass to bio-oil, syngas and biochar in the absence of oxygen. At the present time, research in the downstream processing of bio-oil is progressing (Chen, Andries et al. 2004). Among the different thermochemical conversion routes, gasification has the highest efficiency. Gasification converts biomass, through partial oxidation, to a gaseous mixture

with small quantities of biochar and condensable compounds. Thermochemical gasification is a promising technology that is less restricted to the type of biomass. Gasification takes place at moderately high temperature and turns solid biomass into low to medium heating value combustible gas mixture (known as synthesis gas or syngas) through simultaneous occurrence of exothermic oxidation and endothermic pyrolysis under limited oxygen supply (Faaij 2006; Patwardhan, Brown et al. 2011; Pollard, Rover et al. 2012). In general, a typical gasification system essentially consists of a gasifier unit, a purification system and an energy recovery system. Gasifier reactors are basically classified as fixed beds, fluidized beds and entrained beds. Fluidized bed reactors have an excellent gas-solid contacting leading to very good heat transfer together with the ease of solids handling. Syngas derived from biomass gasification can be burned to generate heat and power or synthesized to produce liquid fuels or valuable chemicals.

Power generation using gasification occurs by combusting the syngas in a gas turbine to provide mechanical work for a generator. Steam is generated by recovering heat from the hot syngas and the steam in turn provides the means for mechanical work via a steam turbine. This gasifier plus gas and steam turbine setup is known as integrated gasification combined cycle (IGCC) power generation. The level of particulates, alkali metals, and tar can decrease the performance of the gas turbine. Consonni and Larson (Consonni and Larson 1996) found that particulate can cause turbine blade erosion and 99% of 10 micron size particles or less should be removed. In addition, they also report that alkali metals corrode the turbine blades and tars condense on the turbine blades both hindering operation and escalating turbine failure. Fortunately, nearly all alkali and tars can be removed using proven wet scrubbing techniques. Using the IGCC approach to generate power, Bridgwater et al. (Bridgwater, Toft

et al. 2002) and Craig and Mann (Craig and Mann 1996) expect biomass to power efficiencies in the range of 35-40% with large scale systems (greater than 100 MW net output) at the high end of the range.

Instead of converting the energy content of the syngas to power, syngas can also be converted into liquid fuels. The conversion of syngas to fuels can only occur in the presence of proper catalysts (Spath and Dayton 2003). The catalytic reactions basically synthesize up the small molecules in the syngas (i.e. carbon monoxide and hydrogen) into larger compounds that are more easily stored and transported. A summary of many catalytic pathways to fuels and chemicals is shown in Fig. 2.1. In most catalytic synthesis reactions, syngas quality requirements are very high. Impurities and contaminants need to be removed. Thus, significant cost must be directed towards syngas cleaning.

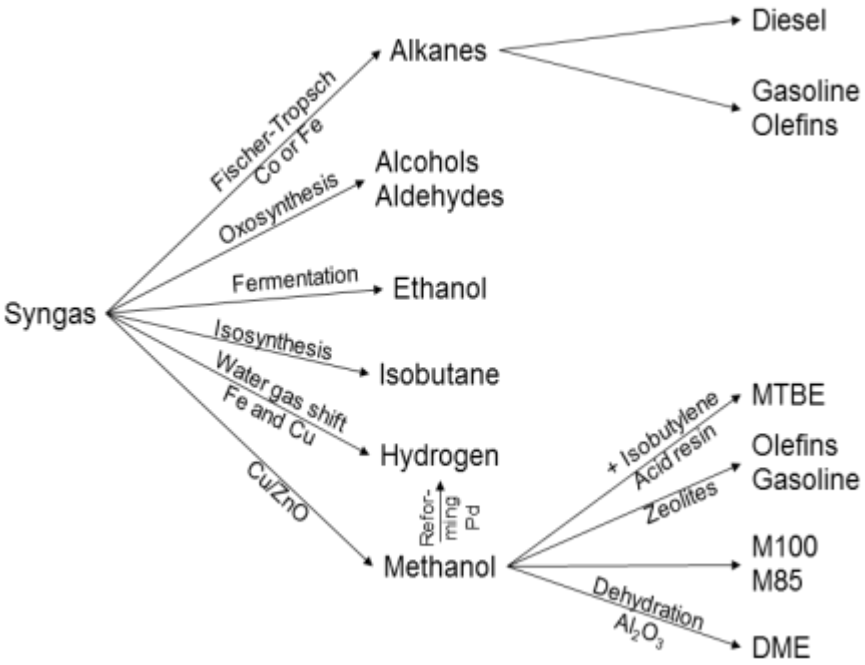

Fig. 2.1. Main syngas conversion pathways (Huber, Iborra et al. 2006)

Fischer-Tropsch synthesis is a feasible way to produce gasoline/diesel range fuels from syngas. It is a highly exothermic reaction producing wide variety of alkanes. For gasoline range products, higher temperatures (300-350°C) and iron catalysts are typically used. For diesel range and wax products, lower temperatures (200-240°C) and cobalt catalysts are typically used (Dry 2002). Product distribution can be estimated using the Anderson-Schulz-Flory chain growth probability model where longer hydrocarbon chains form as the temperature decreases. At around 800 - 900 ^{o}C, the selectivity favors long carbon chain wax products requiring further hydrocracking to the diesel range in a separate unit adding more construction cost, but necessary for liquid fuel production. Due to the highly exothermic reaction, the heat must be removed or the catalyst can be deactivated. Heat removal is crucial to the process and has been the focus of reactor design development (Spath and Dayton 2003).

FT diesel is very low in sulfur, low in aromatic content, and has high cetane number, making it very attractive as conventional fuel alternative. Emissions across the board decrease when using FT diesel. A South African based company, Sasol, has been producing transportation fuel since 1955 using the FT process and supplies 41% of South Africa's transportation fuel requirements (Spath and Dayton 2003).

2.2 Kinetics Modeling

Gasification is a complex phenomenon involving simultaneous heat and mass transfer. Many chemical reactions take place inside the gasifier. These reactions occur simultaneously and the constituents of the product gas are largely dependent on the reaction kinetics and the rate of these reactions. Air, when used as a gasifying agent produces syngas with a lower heating value (4 to 7 MJ/m^3) and it is only applicable for heat and power

generation (Brown 2003). On the other hand, steam and oxygen can produce a better quality of syngas (10 to 18 MJ/m^3). Also, gas constituents (H_2 and CO) are suitable for production of liquid fuels through synthesis process such as Fischer-Tropsch or for production of H_2 that can be used in fuel cells or production of methanol for the chemical industry (Gil 1997). It can also be used for production of fertilizer and generation of electricity (Brown 2003; Basu 2010). Nevertheless, high capital costs and complex system design have precluded steam and/or oxygen gasification as viable for industrial scale (Basu 2010). To overcome these constraints, researchers have looked into using combination of air, steam, and oxygen as gasifying agent. the use of air-steam/oxygen-steam gasification can also offer high gasification efficiency and high gas heating value without the need complex recirculation system (to provide heat for the endothermic steam gasification process) and high capital cost (for pure oxygen) (Brown 2003).

Simulation, or mathematical modeling, of a gasifier is not always a very accurate prediction of its performance, but it provides a qualitative guidance on the design and operating conditions of a gasifier (Lv, Xiong et al. 2004; Lv, Yuan et al. 2007; Huynh 2012). Simulation is important because it allows the plant engineer to optimize the plant with the available experimental data for a pilot plant or current plant (Brown 2003).

Several works on biomass gasification kinetics have been completed previously. Kaushal et al. (Kaushal, Abedi et al. 2010) developed a mathematical model of biomass gasification in bubbling fluidized bed. It is a one-dimensional, two phase (bubble and suspension), two-zone, steady state model. The model, based on global reaction kinetics, mass and energy balances and is capable of predicting temperature and gas concentrations along the reactor's major axis. The model is capable of dealing with wide variety of

biomasses and fluidizing agents, i.e. air, oxygen, steam or a mix of these gases. Researchers have also studied kinetic rate models in case of biomass gasification in great details. Kinetic models provide essential information on kinetic mechanisms to describe the conversion during biomass gasification, which is crucial in designing, evaluating and improving gasifiers. The kinetic model proposed by Wang and Kinoshita (Wang and Kinoshita 1993) is based on a mechanism of surface reactions in the reduction zone assuming a given residence time and reaction temperature. Giltrap et al. (Giltrap, McKibbin et al. 2003) developed a model of the reduction zone of a downdraft biomass gasifier to predict the composition of the producer gas under steady-state operation, adopting the kinetic rate expressions of Wang and Kinoshita (Wang and Kinoshita 1993). Chen (JS 1987) developed a model in order to to estimate the length of the gasification zone and the diameter of the reactor, and to investigate the dependence of the reactor's performance on operating parameters such as feedstock moisture content, chip size, reactor insulation, input air temperature and gasifier load. The main weakness of Chen's model is the over-prediction of the gas exit temperature from the "lumped" zone due to an unrealistically low estimate of heat loss and the omission of CO and H_2 in the pyrolysis gas. Jayah et al. developed a model to address the deficiencies of the Chen model. Sharma (Sharma 2008) presented a model for a downdraft gasifier in which the reduction zone was modelled using a finite rate of reaction following the chemical kinetics. The pyro-oxidation zone, prior to the reduction zone, was also modelled considering thermodynamic equilibrium. However, the author did not take into account any char combustion in the pyro-oxidation zone and also neglected the formation of methane there. Roy et al. (Roy, Datta et al. 2009) developed a model for a downdraft gasifier based on chemical equilibrium in the pyro-oxidation zone and finite-rate kinetic-controlled chemical

reactions in the reduction zone. Several researchers have considered thermodynamic equilibrium models for process modeling and gas composition and important fuel properties. At chemical equilibrium, a reacting system is at its most stable composition, a condition achieved when the entropy of the system is maximised while its Gibbs free energy is minimised. However, thermodynamic equilibrium may not be achieved, mainly due to the relatively low operation temperatures (product gas outlet temperatures range from 750 to 1000 °C) (Bridgwater 1995). Nevertheless, models based on thermodynamic equilibrium have been used widely. Some recent efforts include the work done by Yan et al. (Yan and Zhang 2000), Ruggiero and Manfrida (Ruggiero and Manfrida 1999), Zainal et al. (Zainal, Ali et al. 2001), Schuster et al. (Schuster, Loffler et al. 2001), Altafini et al. (Altafini, Wander et al. 2003).

Some authors, trying to avoid complex processes and develop the simplest possible model that incorporates the principal gasification reactions and the gross physical characteristics of the reactor, have developed models using the process simulator Aspen Plus. Aspen Plus is a problem-oriented input program that is used to facilitate the calculation of physical, chemical and biological processes. It can be used to describe processes involving solids in addition to vapour and liquid streams. This process simulator is equipped with a large property data bank containing the various stream properties required to model the material streams in a gasification plant, with an allowance for the addition of in-house property data. Where more sophisticated block abilities are required, they can be developed as FORTRAN subroutines. Although Aspen Plus has been used extensively to simulate coal conversion, indirect coal liquefaction processes, integrated coal gasification combined cycle (IGCC) power plants, atmospheric fluidised-bed combustor processes and coal gasification

proceses, however, the work that has been done on biomass gasification is less extensive. Mathieu and Dubuisson (Mathieu and Dubuisson 2002) modeled wood gasification in a fluidised bed using Aspen Plus. The model was based on the minimization of the Gibbs free energy and the process was uncoupled in pyrolysis, combustion, Boudouard reaction and gasification. Mitta et al. (N.R. Mitta 2006) modeled a fluidised-bed tyre gasification plant with air and steam using Aspen Plus and validated their results with the gasification pilot plant located at the Chemical Engineering Department of the Technical University of Catalonia (UPC). Nikoo and Mahinpey (Nikoo and Mahinpey 2008) developed a model capable of predicting the steady-state performance of an atmospheric fluidized-bed gasifier by considering the hydrodynamic and reaction kinetics simultaneously. Apart from these, Yan and Rudolph (Yan and Rudolph 2000) developed a model for a compartmented fluidized-bed coal gasifier process, Sudiro et al. (M. Sudiro 2009) modeled the gasification process to obtain synthetic natural gas from pet coke. Biomass gasification modeling is an active area of research in present times and it is a fertile area to explore.

The purpose of this study is to develop a set of multistep kinetics to simulate biomass gasification under various oxygen-steam conditions. Mainly gas phase reactions are studied and solid-gas phase reactions are not taken into account. Detailed mechanisms are not studied to simulate gasification and hence only the main components in syngas such as CO, CO_2, CO, CH_4, H_2O, and N_2 are taken into consideration. The nitrogen present in biomass is converted to NH_3 and HCN during gasification (Brown 2003). Traces of higher alkanes, alkenes like C_2H_2, C_2H_4, C_2H_6 and C_3H_8 are formed as well during gasification (Tian 2007). However, in this study these are not modeled as detailed kinetics mechanisms is not studied. The effects of various feedstocks (corn stover, wood, switch grass etc.) under different

oxygen and steam conditions and quality and heating value of syngas produced from various feedstocks are also taken into consideration in the study to simulate experimental studies performed by Cuong et. al. (Huynh 2012).

This study will focus on bubbling fluidized bed reactors. The fluidized bed gasifier is a very attractive choice for gasification because it can handle a wide range of biomass feedstocks with different compositions (Brown, 2003). Fluidized bed gasifiers are named because of the inert bed material that is fluidized by oxidizing gas creating turbulence through the bed material. Biomass enters just above the top of the bed and mixes with the hot, inert material, thus creating very high heat and mass transfer (Basu, 2010). The gas stream passes vertically upward through a bed of inert particulate matter. This results in a turbulent mixture of gas and solid. The typical operating temperature range in a fluidized bed gasifier is 700 to 850°C, and the bed is expected to have uniform temperature.

The main types of fluidized bed gasifiers are circulating fluidized bed (CFB) and bubbling fluidized bed, which are directly heated from the combustion reactions occurring in the bed. A bubbling bed produces gas and the ash and char falls out the bottom or the side. The CFB recycles the char through a cyclone while the product leaves out the top of the cyclone. Fluidized beds have high carbon conversion efficiencies and can scale up easily (Warnecke 2000). There are certain disadvantages of fluidized bed gasifiers. The effluent temperature is high and this often complicates efficient energy recovery (Brown 2003).

2.3 Geothermal Energy

In addition to bioenergy, geothermal energy is also considered a renewable alternative to fossil energy. Geothermal energy is a thermal energy contained in the crustal rocks and the fluids filling these rocks. It is provided by conduction and convection of heat from the mantle and e the radioactive decay of the minerals in the crust. Geothermal energy can be used in various ways, including (1) direct use for space heating or food processing, (2) heat pumps utilizing the constant year-round temperature at a certain depth underground, and (3) electricity production utilizing dry steam, flash, or binary-cycle power plants. Each geological region has its own geothermal conditions. Various methods to utilize geothermal energy are being employed depending on the available resources and existing demands, e.g., geothermal power plants in volcanic areas or geothermal heat pumps in cold weather regions. For regions with abundant agricultural products, it can be of great interest to combine both biomass and geothermal energy.

Historically, the most common way of capturing geothermal energy was to tap into the naturally occurring hydrothermal convective systems where cooler water enters into the Earth's crust, is heated up, and then rises to the surface. The magnitude of geothermal reserves and their temperature as a function of depth and geographic locations were evaluated (Turcotte 2002). Moderate-temperature water-dominated systems, with temperatures below 130 °C, account for about 70% of the world's geothermal energy potential (DiPippo 2012). The distribution of geothermal energy as a function of the resources temperature and the technical resource potential has been evaluated recently. Binary power cycle technology allows the use of low temperature reservoirs and makes geothermal power production feasible even for countries lacking high enthalpy resources at

shallow depth. For binary power plants two different systems currently are state of the art, the Organic Rankine Cycle (ORC) and Kalina cycle. The binary power plants have the least environmental impact due to the "confinement" of the geofluid. In a binary cycle power plant the heat of the geothermal fluid is transferred to a secondary working fluid, usually an organic fluid that has a low boiling point and high vapor pressure when compared to water at a given temperature. The cooled geothermal water is then returned to the ground by the reinjection well to recharge the reservoir.

This kind of geothermal plant has no emissions to the atmosphere except water vapor from the cooling towers in the case of wet cooling and the loss of working fluid. Thus, environmental problems that may be associated with the exploitation of higher temperature geothermal resources are avoided. The release of greenhouse gases (e.g. CO_2 and CH_4) is of concern. Another advantage of the binary power cycle technology is that the geothermal fluids do not come in contact with the moving mechanical components of the plant (e.g. the turbine), assuring a longer life for the equipment. Binary plants have allowed the exploitation of a large number of fields that may have been very difficult or uneconomic using other energy conversion technologies.

A working fluid in the Organic Rankine Cycle machine plays a key role as it determines the performance and the economics of the plant (Barbier 2002). This justifies the abundant literature dedicated to fluid selection for very different heat recovery applications from which characteristics of good fluids can be extracted (Badr, Probert et al. 1985; Maizza and Maizza 2001; Chen, Goswami et al. 2010; Papadopoulos, Stijepovic et al. 2010). The characteristics are as follows:

• High latent heat of vaporization

• High density of the fluid.

• High specific heat

• Moderate critical parameters (temperature, pressure)

• Acceptable condensing and evaporating pressures

• Good heat transfer properties (low viscosity, high thermal conductivity)

• Good thermal and chemical stability (stable at high temperature)

• Good compatibility with materials (non-corrosive)

• High thermodynamic performance (high energetic/exergetic efficiency)

• Good safety characteristics (non-toxic and non-flammable)

• Low environmental impacts (low Ozone Depletion Prevention, low Global Warming Potential)

• Low cost and good availability

Potential substances identified for ORCs are as follows (Wali 1980; Badr, Probert et al. 1985; Hung 1997; Tchanche, Papadakis et al. 2009; Chen, Goswami et al. 2010):

• Hydrofluorocarbons (HFC)

• Hydrochlorofluorocarbons (HCFC)

• Chlorofluorocarbons (CFC)

• Perfluorocarbons (PFC)

• Siloxanes

• Alcohols

• Aldehydes

• Ethers

• Hydrofluoroethers (HFE)

• Amines

• Fluids mixtures (zeotropic and azeotropic)

The working principle of ORC is simple. The energy and exergy analysis based on the first and second laws of thermodynamics are evaluated for the organic working fluids under diverse working conditions. For simplicity, the internal irreversibility and the pressure drops in evaporators, condensers and pipes are ignored when the thermodynamic properties are calculated. Steady state assumptions are used for analysis. The Rankine cycle consists of the four reversible processes shown in Fig.2.2.

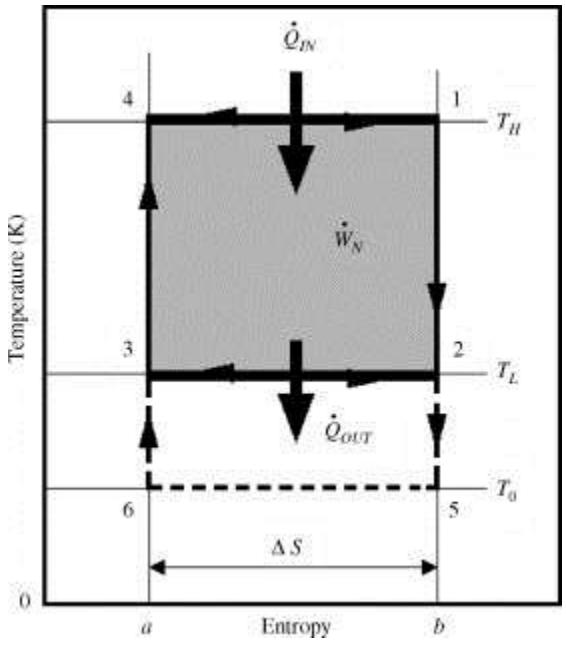

Fig 2.2. Rankine Cycle Working Principle

The processes are

• 1 → 2: Isentropic expansion during which work is produced by the cycle working fluid

• 2 → 3: Isothermal heat rejection from the working fluid to a cooling medium

• 3 → 4: Isentropic compression during which work is performed on the cycle working fluid

• 4 → 1: Isothermal heat addition to the working fluid from a heating medium.

As it is evident from the figure, the temperatures of the heating medium and of the cooling medium are identical to that of the working fluid during the processes 4 → 1 and 2 → 3, respectively. While the working fluid changes from states 4 to 1, the heating medium changes from states 1 to 4, and while the working fluid changes from states 2 to 3, the cooling medium changes from states 3 to 2. This is a practical impossibility for real cycles since there must be a finite temperature difference to drive the heat transfer from one system to the other. Furthermore, the two isentropic work processes (1 → 2 and 3 → 4) are unrealistic; irreversibilities, such as generated from friction, can never be completely eliminated and will cause increases in the entropy, even if the systems are perfectly insulated (another practical impossibility). Thus, real cycles have lower efficiencies than the ideal Rankine cycle. The temperature labeled T_0 is the lowest available temperature of the surroundings, also known as the "dead-state" temperature. It constitutes the lowest temperature that could be used for the heat rejection process, i.e. the lowest sink temperature. The efficiency of such a system is given by the ratio of the total work output from the system to the net energy input into the system. In this study, the refrigerant R134a is used as the organic fluid because it has high specific heat, high latent heat of vaporization and high density.

CHAPTER 3. MODEL FORMULATION

3.1 Aspen Model for Biorefinery

A computer model based on Aspen Plus is created to simulate a biorefinery based on corn stover gasification. The feedstock is purchased at $82.5 per tonne (i.e., metric ton, or 2,200 lb). In the model, corn stover is first pretreated where it is dried from 25% to 8% moisture level and then grinded to small pellets for gasification. It is then sent for gasification in a fluidized bed gasifier. The syngas out of the gasifier contains impurities and hence it is routed for cleanup. The next step is the catalytic synthesis of syngas to produce a mixture of hydrocarbons which are further refined to produce transportation fuels. The unconverted syngas and biochar is combusted and used for heat or power generation.

The following steps are taken in performing this study. (1) Using the criteria described in Scenario Selection, a gasification scenario is selected for detailed analysis. (2) A process model for this scenario is developed using Aspen Plus. (3) Equipment lists are generated and unit costs are evaluated using literature sources and Aspen Icarus Process Evaluator. (4) Capital investments are estimated and the fuel product value (PV) at zero net present value and 10% internal rate of return (after tax) is determined for the n^{th} plant. (5) The analysis for the pioneer plant is conducted to estimate the capital investment and product value for the first plant of its kind.

3.1.1 Scenario Selection

A fluidized bed gasifier is considered in this study. Advantages of fluidized bed gasification include simple construction and operation, lower capital cost, and high heat transfer rates within the bed, uniform temperature distribution, and better gas-solid

contact(Swanson, Platon et al. 2010). The proposed gasification biorefinery is chosen considering that (1) the technology is feasible in the next decade and there is a high scope of technology development, (2) the size of the biorefinery is probable with the current agricultural input, and (3) the end products are compatible with the existing fuel infrastructure, i.e., gasoline and diesel fuel.

There are uncertainties in commercial readiness for hot gas cleaning, e.g., catalytic tar cracking. Thus, cold gas cleaning (i.e. direct quench water scrubbing) is chosen in this study. Fischer-Tropsch (FT) catalytic synthesis is chosen for fuel production because it is a relatively mature technology. Gasoline and diesel fuel, being supported by the FT synthesis, are the main products of the biorefinery. The plant size is chosen to be 2,000 tonnes per day based on previous studies (Damartzis and Zabaniotou 2011). This feed rate is also consistent with the feasible agricultural residue outputs in the Midwest region of the U.S. at the assumed feedstock delivery price.

3.1.2 Process Design

It is assumed that corn stover (25 wt% moisture and 6% ash content) is purchased at $82.5 per tonne. The transportation cost and payment for the grower are included in the cost. Figure 3.1 shows the main operational areas considered in the model. A summary is listed below and more detailed descriptions are provided in the following sections.

i) Preprocessing – In this section the feedstock is dried from 25% to 8% moisture content and then grinded to small pellets for gasification

ii) Gasification – The feedstock is pressurized and sent to the gasifier to produce medium energy content syngas.

iii) Syngas cleaning – The pollutants present in the syngas are removed and the syngas is cooled subsequently.

iv) Fuel synthesis – By the FT process, syngas is catalytically converted to a mixture of hydrocarbons.

v) Hydroprocessing – The mixture of hydrocarbons are further treated to produce transportation fuels.

vi) Power generation – Unconverted syngas is burned to produce electricity

vii) Air separation unit – Pure oxygen is provided for gasification after the separation of nitrogen from air.

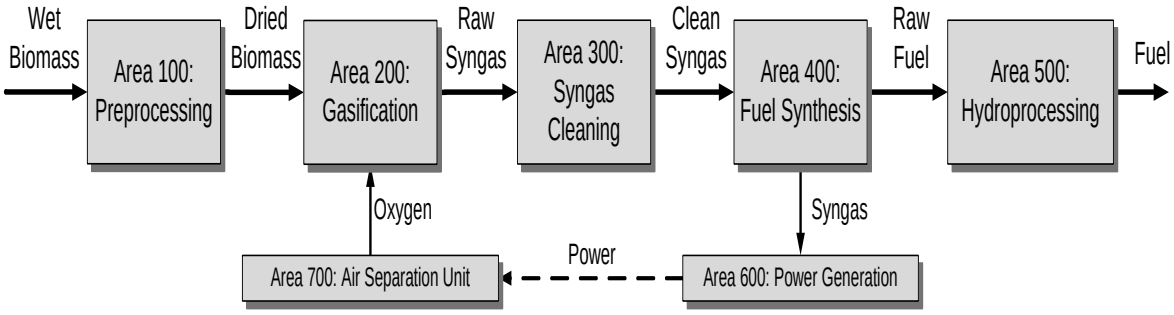

Figure 3.1. Overall process flow diagram of the present gasification biorefinery

From previous studies, it is assumed that the plant is available at 85% capacity (7,446 hours per year). This assumption is feasible for the n^{th} plant. The detailed process flow diagram for the entire process is shown in Fig. 3.2.

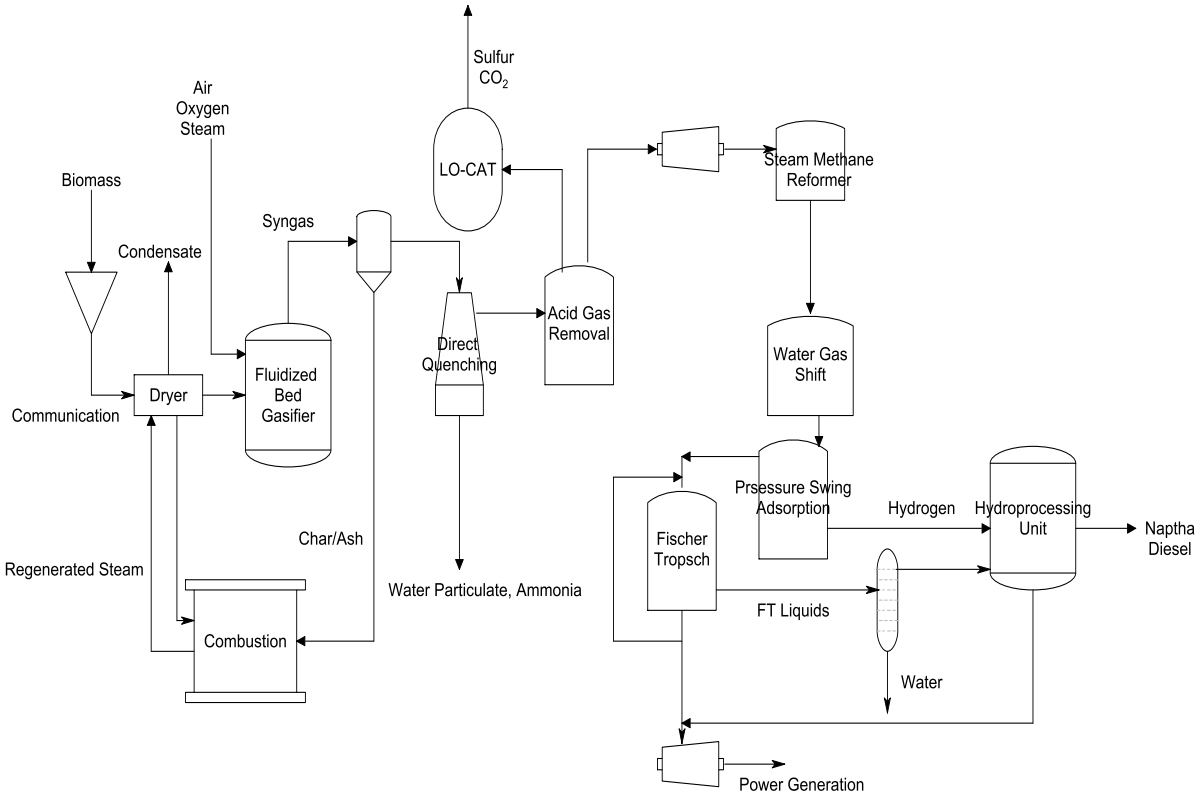

Figure 3.2. Detailed process flow diagram

Recycled streams are utilized to provide better FT products conversion. Unconverted syngas in the fuel synthesis area is recycled to the syngas cleaning area to remove carbon dioxide and allows for further conversion in the Fischer-Tropsch reactor. The balance of unconverted syngas is combusted in a gas turbine and waste heat is recovered in a steam generator for steam turbine power. Power generated is used throughout the plant and excess is sold. Unconverted carbon within the gasifier in the form of char is collected and combusted in a furnace to produce heat thereby generating steam for the drying of the biomass.

3.1.3 Preprocessing

In this section, the raw biomass is processed to 6-mm pellets and the moisture level is reduced from 25% to 8%. The size reduction procedure includes both the primary and secondary reduction steps, and correlations are used to calculate the power required for the particle size reduction (Tijmensen, Faaij et al. 2002). The performance of a gasifier depends on the size and moisture of the feedstock. Pellet size of 6 mm and moisture content of 8% are appropriate for gasification. The corn stover composition is shown below in Table 3.1. Ash content is assumed to be 6% by weight. Char composition, formed in the gasifier, is also shown in Table 3.1. Forklifts transport the bales to conveyors where the stover is separated from any metal in a magnetic separator. The first modeled operational area is a primary biomass chopper to complete the initial size reduction step and prepare stover for drying.

Table 3.1. Stover and char elemental composition (wt. %)

Element	Stover	Char
Ash	6.00	0
Carbon	47.28	68.05
Hydrogen	5.06	3.16
Nitrogen	0.80	0.29
Chlorine	0	0
Sulfur	0.22	0.15
Oxygen	40.63	28.34

The next area of operation is the direct contact steam drying which is modeled as a rotary steam dryer with exiting biomass moisture of 10% on wet basis. For the drying of biomass from 25% to 8% moisture content, 15000 metric tons per day of steam is required based on previous study (Mani 2004). These 15000 metric tons per day steam is utilized in a loop and heated to 200°C from the hot combustion flue gases exiting the syngas or char fired

combustor and natural gas combustion. Steam mixes with 25°C biomass and enters the drier. At the exit, steam at 120°C returns to the combustor for reheating and dried biomass exits at 90°C and is conveyed to the grinding area.

The grinding area is the same configuration as the chopping area except the grinder requires significantly more power due to the larger size reduction. The grinder reduces the size of the biomass to 6 mm. The power required for grinding the biomass into short pellets is 1100 kW. Energy requirements for grinding are determined using the correlations for specific energy (kWh per short ton) which has been adapted from literature (Amos 2008).

3.1.4 Gasification

The gasification area of the plant produces synthesis gas using pressurized gasifiers. Also in this area slag, char, and ash are removed. This area also includes lock hoppers for biomass pressurization and a fired combustor which provides heat to raise steam for drying the stover. Dried and ground stover enters the area and is immediately conveyed to a lock hopper system for pressurized feeding. Carbon dioxide is used as pressurization gas and arrives from the syngas cleaning area. According to literature (Mani 2004), a lock hopper system is the best setup for pressurized feeding of solids, despite higher operating costs due to high inert gas usage. The power requirement of a lock hopper system using biomass is 0.082 kW/metric ton/day resulting in a 180 kW system.

A fluidized bed gasifier is used in this study. Gasification using air produces a low heating value syngas (4 to 7 MJ/Nm^3) that is only suitable for heat and power generation (Lau, Bowen et al. 2002). On the other hand, steam and oxygen can increase the heating value of syngas to 10 – 14 MJ/Nm^3 as well as raise the concentration of main gas constituents of H_2 and CO that are suitable for liquid fuels production through the FT

synthesis (Gil 1997; Sethuraman, Van Huynh et al. 2011; Huynh 2012). The fluidized bed gasifier operates under pressurized conditions using steam and 95% pure oxygen. Based on the biomass feed rate, 352 tonne/day of steam and 540 tonne/day of oxygen are required. The system also includes lockhoppers to pressurize the biomass. A lockhopper system is the most appropriate system for pressurized biomass feeding despite the high cost due to the use of inert gas (Damartzis and Zabaniotou 2011; Huynh 2012). Carbon dioxide is used as the pressurization gas to avoid the dilution of nitrogen in the downstream equipment. Carbon dioxide is obtained from the downstream acid gas removal area. The gasifier operates at a pressure of 28 bars and 870 °C. The mass ratio of oxygen to biomass entering the gasifier is 0.26. Furthermore, steam addition to the gasifier is set at 0.17 mass ratio of steam to biomass (Lau 2002). Solids and particulate matter such as slag, biochar and ash are removed from the bottom of the gasifier. The gasifier uses a 0.26 mass ratio of oxygen to biomass at a gasification temperature of 870°C. This ratio is developed from the data found in an IGT gasifier study by Bain (Swanson, Platon et al. 2010). In that study, Bain develops mass balances for an IGT gasifier operating with woody biomass. Steam addition to the gasifier is calculated using a 40/60 steam to oxygen mass ratio consistent with experiments performed at Iowa State University using corn stover feedstock and a steam/oxygen blown, fluidized bed gasifier.

In absence of a detailed kinetic model of gasification, experimental data on syngas composition from a laboratory-scale gasifier and the principles of mass conservation are used to calculate the gas yield in the process model (Bain 1992). This method is used also because low-temperature gasification cannot be modeled using equilibrium assumption. The RYIELD model in Aspen Plus is employed to determine syngas composition. The syngas composition

obtained from the model is given in Table 3.2. In the model, biochar is also considered in calculating the carbon balance. Hydrogen and water are included in hydrogen balance. Lastly, oxygen balance is determined by also considering carbon monoxide and carbon dioxide, in addition to water. Directly after the gasifier initial syngas cleaning occurs whereby cyclones capture char and ash. The cyclones are split into two trains because of high volumetric gas flow. Each train contains a medium efficiency followed by high efficiency cyclones particulate capture. Overall particulate removal efficiency for cyclone area is 99%. Nearly particulate-free syngas travels to the more rigorous syngas cleaning area. In this study, the biochar and ash are collected using a cyclone separator and sent for combustion in a fluidized bed combustor to provide part of the heat to regenerate steam for feedstock drying. The combustor is assumed to operate adiabatically resulting in an exit flue gas temperature of approximately 1800 °C. Hot flue gas heats 120°C steam to 200°C and loops to the stover drying area. The resulting syngas has an energy content of 10 MJ/Nm^3.

Table 3.2. Syngas composition (mole basis) leaving gasifier

Component	**Composition (mole fraction)**
Carbon Monoxide	0.230
Hydrogen	0.210
Carbon Dioxide	0.264
Water	0.204
Nitrogen	0
Methane	0.055
Ethane	6100 ppm
Ethylene	0.013
Ammonia	9400 ppm
Hydrogen Sulfide	1120 ppm
Tar (Anthracene)	500 ppm
Argon	0.006

3.1.5 Syngas cleaning

After the initial particulate removal accomplished by the cyclones, the syngas still contains some particulate and all of the ammonia, hydrogen sulfide, and other contaminants. The species are removed using a cold gas cleaning approach, which is presently proven in many commercial configurations. Hydrogen sulfide and carbon dioxide, collectively known as acid gas, is absorbed via amine scrubbing. Hydrogen sulfide and carbon dioxide, collectively known as acid gas, is absorbed via amine scrubbing. Separation of carbon dioxide from hydrogen sulfide with subsequent recovery of solid sulfur occurs via the LO-CAT® hydrogen sulfide oxidation process.

Due to less than optimal hydrogen to carbon monoxide ratio from the gasifier, a water-gas-shift (WGS) reaction is necessary at some point in the process to adjust to optimum Fischer-Tropsch ratio of 2:1. A significant WGS activity is required meaning a sizable amount of carbon dioxide is produced. To keep that carbon dioxide from building up in downstream processes, the sour water-gas-shift (SWGS) reactor is located before the acid gas removal area. In this scenario, In the scenario, the direct quench unit condenses the syngas removing approximately 90% of ammonia and 99% of solids. Tar is condensed in this unit and can be recycled back into the gasifier using a slurry pump, but this configuration is not modeled. A water treatment facility for the direct quench effluent is not modeled, but is accounted for in a balance of plant (BOP) cost.

The next cleanup step is the removal of the acid gases (carbon dioxide and hydrogen sulfide) through the use of an amine-based solvent in a chemical gas absorption system. At this point in the cleaning process, hydrogen sulfide and carbon dioxide content is

approximately 900 ppm and 30% on molar basis, respectively. Sulfur must be removed to at least 0.2 ppm for Fischer-Tropsch synthesis (Swanson, Platon et al. 2010). According to the GPSA Engineering Data book(DC December, 2003), amine-based systems are capable of removing sulfur down to 4 ppm. Therefore, a zinc oxide guard bed is required to remove the difference. In this study, 20% concentrated monoethanolamine (MEA), capable of absorbing 0.4 mol acid gas per mole amine, is used as the absorbent. The process setup is based on report by Nexant Inc. Hydrogen sulfide leaves the top of the absorber at 4 ppm and CO2 at 2%, which is 99% and 90% removal, respectively. The clean syngas is now ready for polishing to final cleanliness requirements. A stripper is utilized to desorb the acid gas and regenerate the amine solution. Before the acid gas and amine solution enter the stripper a heat exchanger raises the temperature to 90°C.

Acid gas is brought to the LO-CAT sulfur recovery system to isolate hydrogen sulfide and convert it to solid sulfur. The LO-CAT system sold and owned by Gas Technology Products uses oxygen and a liquid solution of ferric iron to oxidize hydrogen sulfide to elemental solid sulfur (Inc. 2006). This system is suitable for a range of 150 lbs to 20 ton per day sulfur recovery and also 100 ppm to 10% H_2S concentration in sour gas as reported by Nexant Inc.(Merichem). The sulfur production in this model is approximately 3 metric ton per day and H_2S concentration approximately 150 ppm which is within the reported ranges. First, the H_2S is absorbed/oxidized forming solid sulfur and water while the ferric iron converts to ferrous iron. The second vessel oxidizes the ferrous iron back to ferric iron and the sulfur cake is removed while the iron solution is recycled back into the absorber (Inc. 2006). The carbon dioxide gas stream from the absorber is split where a portion is compressed and used in biomass pressurization while the rest is vented to the atmosphere.

3.1.6 Fuel Synthesis

The conversion from syngas to liquid fuel occurs in the fuel synthesis section. The major operations are zinc oxide-activated carbon gas polishing, syngas booster compression, steam methane reforming, water-gas shift, hydrogen separation via Pressure Swing Adsorption, FT synthesis, FT product separation, and unconverted syngas distribution. The scenario contains the water-gas-shift reaction and steam methane reformer since recycle streams contain high enough content of methane and ethylene to significantly accumulate and cause dilution.

A compressor is used in the fuel synthesis section to boost up the pressure to 25 bar for FT synthesis. Then the syngas is heated to 200°C and passes through zinc oxide/activated carbon fixed bed sorbent. To limit downstream catalyst poisoning, the syngas steam must be cleaned of these components. Removal to 50 ppb sulfur is possible with zinc oxide sorbent (Kohl and Nelson 1997). To comply with reported requirements the sorbent removes sulfur to approximately 200 ppb. In addition to sulfur, halides are removed by the sorbent. Syngas contaminant level requirements for Fischer-Tropsch synthesis are shown in Table 3.3.

Table 3.3. Fischer-Tropsch gas cleanliness requirements (Inc. 2006)

Contaminant	Tolerance Level
Sulfur	0.2 ppm (200 ppb)
Ammonia	10 ppm
HCN	10 ppb
Halides	10 ppb

Methane, nitrogen and carbon dioxide act as inerts in the FT synthesis. At this point, a steam methane reforming (SMR) step is utilized. Syngas is heated to 870°C through a fired heater and passed through a reformer nickel-based catalyst to reduce methane, ethylene, and

ethane content. It is assumed that the SMR can be modeled to operate at equilibrium. Steam is added to bring the steam to methane ratio to approximately 6.0 which at 870°C and 26 bar results in about 1.5% equilibrium methane content in exit stream (Spath and Dayton 2003). The WGS reaction is now employed in order to increase the H_2: CO ratio.

The exiting H_2/CO ratio after WGS is slightly above 2.1 in order for the excess hydrogen to be separated and used in the hydroprocessing area. A pressure swing adsorption (PSA) process is employed to isolate a stream of hydrogen. Since only a small amount of hydrogen needs to be separated from the syngas stream for downstream use, a small percentage of the syngas is directed to the PSA unit. Hydrogen removal efficiency within the PSA unit is assumed to be 85% and produces pure hydrogen (Imperial Chemical Industries 1970). After the PSA, the syngas rejoins the main gas line and enters the FT reactor. The Fischer-Tropsch synthesis reactor operates at 200°C and 25 bar using a cobalt catalyst. Per pass carbon monoxide conversion in the reactor is set at 40%. The product distribution follows the Anderson-Schulz-Flory alpha distribution.

3.1.7 Hydroprocessing

Due to the FT synthesis, a considerable amount of waxes are formed in the liquid. These waxes are hydrocracked in a hydroprocessing unit. This requires hydrogen in order to crack high molecular weight parrafins to low molecular weight hydrocarbons. Hydrogen is obtained from the fuel synthesis section and is recycled within the hyrdoprocessing unit as needed. The hydroprocessing area contains a hydrocracker for converting the wax fraction and a distillation section for separating naphtha, diesel, and lighter molecular weight hydrocarbon. Methane and LPG are separated and used to fuel the gas turbine in the power generation area. The hydroprocessing area is modeled as a "black box." In the model, 61%

diesel fuel and 27% naphtha are obtained from this section. The remaining 12% comprises of gaseous hydrocarbons which are used as fuel for the gas turbine for power generation. These liquid fuels are then used as blend stock for gasoline and diesel fuel.

3.1.8 Power Generation

A gas turbine and steam turbine provide the means to producing power that is required throughout the plant and also generate excess power for export. Unconverted syngas from the fuel synthesis section and fuel gas from the hydroprocessing unit are burned in a gas turbine. Much of the exhaust heat is recovered via steam generators, and the steam is sent to the steam turbine where additional power is generated. A portion of the power generated is used in the plant and the remaining is sold. Thus, this biorefinery is self-sustained as there is no need to purchase power from outside.

3.1.9 Air Separation Unit

In this study, 95% pure oxygen is supplied for gasification. An air separation unit (ASU) is used. The unit is based on a two-column cryogenic oxygen/nitrogen separation system. Pre-cooling of air is accomplished by the exchange of heat with the exiting nitrogen from the separation unit. This area requires a significant amount of power. The air separation unit uses power that is generated in the present biorefinery.

3.1.10 Geothermal Steam Integration

Geothermal energy can be utilized in various ways. Geothermal energy is extracted in the form of liquid at the wellhead. In this study, heat is extracted from geothermal fluid at the wellhead through heat exchanging processes and used to generate steam for use in the biorefinery. The term “geothermal steam” will be used in this paper to represent such steam. As a result, geothermal steam is integrated into the biorefinery via direct use and electricity

production. In the original setup of the biorefinery, process steam is used for drying the biomass, gasification, and steam-methane reforming. In the integrated system, the feasibility of replacing the process steam with geothermal steam is explored. It is found that geothermal steam can be used successfully to replace the purchased steam for gasification and steam-methane reforming. A preliminary study shows that it is not cost-effective to use the present geothermal steam for biomass drying (Swanson, Platon et al. 2010). To dry the biomass to the desirable moisture level at the current feed rate, 15,000 tonnes of steam is required according the previous study (Banerjee, Tiarks et al. 2011). This steam is purchased once. During drying, the steam temperature drops from 200 to 120 °C. This steam is then recycled and reheated using energy generated from combustion of biochar and natural gas. On the other hand, gasification and steam reforming consume steam continuously at 352 and 1,000 tonnes/day, respectively. These two streams of steam are replaced by geothermal steam in this study. Additionally, unused geothermal fluid is used to produce electricity as a byproduct of the biorefinery via a binary cycle.

3.2 Gasification Kinetics Model

In this study two methods of modeling biomass gasification are investigated. In the baseline case, a mass balance approach is taken to model the process flow of an experimental, pilot-scale gasifier. In the second case, a set of multistep kinetics model is developed to simulate biomass gasification under various oxygen-steam conditions using different feedstock. The present model is validated using experimental data obtained under various feedstock and operating conditions.

3.2.1 Model Formulation

A typical biomass gasification process includes the following steps: drying, pyrolysis, partial combustion of some gases, vapors and char, and gasification of decomposition products. This section will describe the two methods taken to model a pilot-scale gasifier under various feedstock and operating conditions. Section 3.2.1.1 describes the experimental setup and results that will be modeled. Section 3.2.1.2 describes how the mass balance approach to modeling this data is accomplished while Section 3.2.1.3 provides the details of the kinetic modeling of the gasifier. The biomass gasification models are set up using Aspen Plus and consist of a biomass feeding system, liquid oxygen supply, steam generation unit, and a fluidized bed gasifier as illustrated in Fig 3.3. The chars produced are collected and can be used for varied purposes such as combustion for heat generation or as an agricultural product to enrich soil.

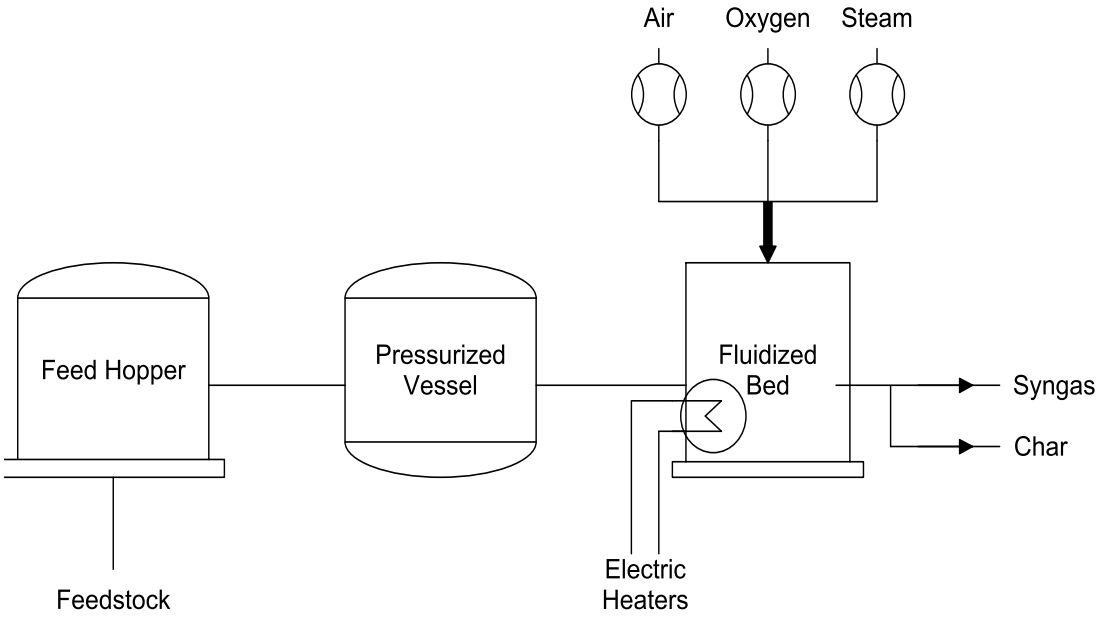

Fig. 3.3. Schematic of the gasification system model

3.2.1.1 Experimental Setup and Data Collection

A fluidized bed biomass gasifier is used for experiment. This gasifier has the capability to operate at a temperature of 815°C, a pressure up to 50 psig, and the ability to use pure air or oxygen-enriched air with various steam additions as the gasifying agent (Sethuraman, Van Huynh et al. 2011; Huynh 2012). This system is rated for approximately 800 kW, corresponding to 180 kg/hr feed rate of raw biomass with an average heating value of 16,000 kJ/kg (Huynh 2012). Tests are conducted for five different kinds of biomass and four different oxygen concentrations in the gasifying medium. Therefore, twenty different sets of syngas are obtained. The proximate and ultimate analyses of the feedstock are given in Table 3.4.

Table 3.4 Proximate and Ultimate Analysis of Feedstocks (Huynh 2012)

Feedstock	Wood (Maple-Oak)	Char (Maple-Oak)	Wood (pine)	Corn Stover	Seed Corn	Switch Grass
	Proximate Analysis (Wt%)					
Volatiles	75.11	-	74	66.63	66.43	69.37
Fixed Carbon	16.81	-	16.66	15.12	17.15	14.47
Moisture	6.25	-	8.9	5.25	15.01	14.23
Ash	1.83	-	0.43	13.01	1.4	1.93
	Ultimate Analysis (Wt%)					
C	46.56	63.05	47.52	46.8	40.07	49.09
H	6.24	0.71	6.5	5.1	7.1	5.88
N	0.14	0.29	0.05	0.6	1.4	0.18
O	46.13	35.91	46.36	47.32	50.5	44.75
S	0.02	0.04	0.01	0.1	0.17	0.1

The amount of steam added to the gasifying agent is determined by the amount required to keep a constant bed temperature as additional oxygen is added to the flow. As seen in Table 3.5, the steam-to-oxygen ratio (S/O) increases with higher oxygen concentrations in the flow.

Table 3.5 Operating conditions (Huynh 2012)

Feedstock	**Maple-Oak**			**Pine**			**Seed Corn**		
Oxygen Percent (Wet Basis)	21	30	40	21	30	40	21	30	40
Oxygen Percent (Dry Basis)	21	45	80	21	45	80	21	45	80
Bed Temperature (°C)	800	800	800	800	800	800	800	800	800
Biomass (lb/hr)	250	345	370	190	290	350	190	290	375
Air (lb/hr)	275	117	31	202	94	29	202	94	32
Steam (lb/hr)	0	52	67	0	49	59	0	49	65
Oxygen (lb/hr)	0	51	82	0	48	73	0	48	81
ER	0.15	0.13	0.14	0.14	0.13	0.13	0.15	0.15	0.14
S/O	0	1.18	1.31	0	1.25	1.32	0	1.25	1.31
O/B	0.2	0.39	0.45	0.2	0.43	0.42	0.23	0.5	0.51

3.2.1.2 Baseline Model for the Gasification System

A baseline model using a mass balance approach to determining the product yield is developed in Aspen Plus to simulate the present gasification system using maple-oak mixtures, which are ground and prepared as cylindrical pellets. The model is applied to

simulate the system performance using air blown with a bed temperature of 815 °C. In the present model, a feed hopper containing the biomass at a 6% moisture level supplies feedstock to a pressurizing vessel before entering the gasifier with outputs of syngas and char. Due to the relative low-temperature conditions of this model, the equilibrium kinetic assumption built into Aspen Plus cannot be applied. Therefore, an approach which aims to balance the flow of each element into and out of the gasifier is employed. (Swanson, Platon et al. 2010). The present approach utilizes the built-in RYIELD model in Aspen Plus with a correction programmed using a Fortran code. In order for this method to be effective, experimental data including the syngas composition and yield as well as the feedstock and char ultimate and proximate analyses are supplied to the model. This requirement makes the baseline model less predictive of various feedstock and operating conditions than a detailed kinetics model; however, it is still valuable when evaluating the overall plant energy flows and downstream processes of the gasifier.

The approach taken to balance each element (carbon, hydrogen, oxygen, sulfur, nitrogen, and ash) is to have a "floating" component for each element. This component's yield is adjusted in order to meet the demands of the rest of the process. For example, char is used to "float" carbon. If there is insufficient carbon in the other process streams, less char is produced and the excess carbon is distributed where needed. After carbon is balanced, the calculation proceeds to sulfur and nitrogen balances, with any excess being converted to form hydrogen sulfide and ammonia. Next, elemental hydrogen is adjusted to fit the operating conditions by either converting diatomic hydrogen to steam or decomposing steam to diatomic hydrogen. A scaling factor can be implemented in this step to determine the

amount of diatomic hydrogen that is converted to steam to best match experimental results. Finally, oxygen is balanced by adjusting the amount of CO_2 and CO which exits the gasifier.

3.2.1.3 Gasification Kinetics Development

In this study it is assumed that the biomass pyrolyzes immediately after entering the gasifier and produces a mixture of gases, liquids and solids (char). Then, for simplicity it is assumed that gas phase reactions (cracking, reforming, combustion, water-gas shift, etc.) occur among the pyrolytic products as well as the gasification agents, and syngas is produced. Several cases are studied with a variety of biomass and oxygen-steam ratios. Several different kinds of biomass, such as pine, maple-oak, seed corn, switchgrass, and corn stover, are modeled in the study to test the validity of the proposed biomass gasification kinetics. The present reaction kinetics is implemented into the gasification module of Aspen Plus, and the following assumptions are made.

i) The process is steady-state and isothermal in nature.

ii) The devolatilization process takes place immediately and the product mainly consists of H_2, CO, CO_2, CH_4, and H_2O.

iii) Char formed during the gasification process consists of carbon and ash.

iv) The gases are uniformly distributed in the emulsion phase.

The present kinetics model considers the following important reactions to simulate biomass gasification.

$CO + H_2O = CO_2 + H_2$ $\qquad k_f = 2.84 * 10^{-2} \exp\left(-\frac{3961}{T}\right)$ (1)

$H_2O + C = CO + H_2$ $\qquad k_f = 2.07 * 10^{7}\, exp\left(-\frac{3940}{T}\right)$ (2)

$C + 2H_2 = CH_4$ $\qquad k_f = 4.18 * 10^{-3} \exp\left(-\frac{2317}{T}\right)$ (3)

$CO_2 + C = 2CO$ $$k_f = 1.12 * 10^8 \exp\left(-\frac{26927}{T}\right) \quad (4)$$

$H_2O + CH_4 = CO + 3H_2$ $$k_f = 7.301 * 10^{-1} \exp\left(-\frac{36.15}{T}\right) \quad (5)$$

The above reaction equations are solved using the constantly stirred tank reactor model in Aspen Plus known as RCSTR. CSTR is continuously stirred tank reactor. In a CSTR there is a continuous flow through the reactor and the contents of the reactor are ideally mixed or in other words the effluent composition is the everywhere in the reactor. Since these are not elementary reactions, each reaction can be considered as a series of multiple and complex stages. A chemical reaction can be treated as the simultaneous occurrence of the forward and backward reaction. These forward and backward reactions occur at different rates, thus favoring the reaction in a particular direction. The rates of the reactions are strong functions of the concentrations of the species. The relation between the forward and backward reactions is given by

$$K_e = k_{forward}/k_{backward} \quad (6)$$

where the equilibrium constant $K_e = exp(-\Delta G_0/RT)$ (G_0 is the Gibbs free energy).

CHAPTER 4. ECONOMIC ANALYSIS

The total capital investment, operating costs, and product values are estimated considering an operating duration of 20 years for the plant. The total equipment costs, the installation costs, and the indirect costs (such as engineering, construction, and contingency costs) sum up to the total capital investment. The total annual operating cost is calculated and a discounted cash-flow rate of return (DCFROR) analysis is developed. The rate of return on investment is fixed at 10%. The product value (PV) (i.e., levelized product cost) per gallon of gasoline equivalent (GGE), based on energy, is determined at a net present value of zero given to this rate of return. All the financial data are reported for the 2012 cost year. The major economic assumptions used in this analysis are listed in Table 4.1.

Table 4.1. Main economic assumptions for n^{th} plant scenarios

Parameter	Assumption
Financing	100% equity
Internal rate of return (after taxes)	10%
General plant depreciation period	7 years
Steam plant depreciation period	20 years
Construction period	2.5 years with total capital investment spent at 8%, 60%, and 32% per year during years before operation
Startup time	0.5 years where during that time revenues, variable operating costs, and fixed operating costs are 50%, 75%, and 100% of normal, respectively.
Income tax rate	39%
Contingency	20% of fixed capital investment
Electricity cost	6 cents/kWh
Working capital	15% of fixed capital investment
Land purchase	6% of total purchased equipment cost
Plant availability	310 days per year (85%)

The various equipments employed in the model are sized, and the costs are estimated using data from literature and the Aspen Process Economic Evaluator, also known as Aspen Icarus. Unique equipment costs for such equipment as the gasifier and Fischer-Tropsch synthesis reactor are estimated externally using literature references (Amos 2008). Additionally, some equipment such as the biomass dryer and lock hoppers require literature references to determine the sizing whereby their costs are subsequently estimated using Aspen Process Economic Evaluator. The hydroprocessing plant area is modeled as a "black box" and therefore its costs are estimated as an overall scaled area cost from literature. To scale the equipment of different sizes, Eq. (4.1) is used by considering the initial equipment cost ($Cost_0$). A scaling factor, *n*, typically ranging from 0.6 to 0.8, is used (Larson 2005.).

$$Cost_{new} = Cost_0 * \left[\frac{Size_{new}}{Size_0}\right]^n \quad (4.1)$$

All purchased equipment costs determined via Aspen Process Economic Evaluator contain an installation factor that accounts for piping, electrical, and other costs required for installation. However, this installation factor tends to be significantly lower than metrics suggested by Peters et al.(Swanson, Platon et al. 2010) Therefore, rather than using the software-derived installation factors, an overall installation factor is applied to most equipment. A 3.02 overall installation factor is used as suggested by Peters et al. for solid-liquid plants. The purchased equipment cost of a piece of equipment is multiplied by the installation cost to determine its installed cost. For the gasification unit, a 2.35 installation factor is used according to a National Energy Technology Laboratory study (Peters, Timmerhaus et al. 2003). It is assumed that all gas compressors receive a 1.2 installation factor which is consistent with Aspen Process Economic Evaluator. For multiple unit

operations that operate in parallel or in trains, a train cost factor is applied. The reason for the factor, as reported by literature (Reed, Van Bibber et al. 2007), is because those units share some of piping, electrical, and other installation costs. In the preprocessing and gasification sections, there are several units operating in parallel. Thus, an overall train cost is evaluated using Eq. (4.2) (Larson, Jin et al. 2009)

$$Cost_{train} = Cost_{unit} * n^{m} \quad (4.2)$$

Here, n is the number of units and m is the train factor, with m = 0.9 due to shared installation materials costs (Larson 2005.). Using the Aspen Economic Evaluator, the total purchased equipment costs (TPEC) and Total Installed Costs (TIC) are determined. Then, the Indirect Costs are estimated based on TPEC. Methods to obtain the total capital investment are summarized in Table 4.2. Indirect costs (IC) include those for engineering and supervision, construction expenses, and legal and contractor's fees at 32%, 34%, and 23% of TPEC, respectively. The Total Direct and Indirect Cost (TDIC) is the sum of Total Installed Cost (TIC) and Indirect Cost (IC). Project contingency is added as 20% of TDIC. The Fixed Capital Investment (FCI) is the sum of TDIC and project contingency. Total Capital Investment (TCI) is obtained by adding the working capital (15% of FCI) to FCI and it represents the overall investment required for each scenario. The equipment installation costs are consistent with the methodology used in literature (Banerjee, Tiarks et al. 2011).

Table.4.2 Capital cost estimation for the n^{th} plant scenario

Parameter	**Method**
Total Purchased Equipment Cost (TPEC)	Aspen Icarus Process Evaluator
Total Installed Cost (TIC)	TPEC × Installation Factor
Indirect Cost (IC)	89% of TPEC
Total Direct and Indirect Costs (TDIC)	TIC + IC
Contingency	20% of TDIC
Fixed Capital Investment (FCI)	TDIC + Contingency
Working Capital (WC)	15% of FCI
Total Capital Investment (TCI)	FCI + WC

Raw material costs are inflated using the Industrial Inorganic Chemical Index also used by Phillips et al. Variable operating costs and respective cost method is shown in Table 4.3. Natural gas for use in the gas turbine to produce power during startup and backup periods is assumed to be employed 5% of the annual operating time. Wastewater disposal cost is applied to the sludge and black water produced during direct syngas quench. The cost of the catalysts is not calculated for each year. It is assumed that the catalysts are replaced after every 3 years. Salaries are calculated similarly to Phillips et al. (Peters 2003) where employees include a plant manager, shift supervisors, lab technician, maintenance technician, shift operators, yard workers, and office clerks. Overhead is calculated as 60% of total salaries; maintenance cost and taxes/insurance cost are both 2% of total installed equipment cost as in accordance with Aden et al. (Statistics 2008).

Table 4.3. Operating Cost Parameters

Category	**Cost information**
Feedstock	$82.5/tonne
LO-CAT Chemicals	$176/tonne of sulfur produced (Aden, Ruth et al. 2002)
Amine make-up	$1.09/lb and set as 0.01% of the circulating rate (Phillips, Aden et al. 2007)
Process Steam	$9.02/tonne (Phillips, Aden et al. 2007)
Cooling water	$0.34/tonne (Peters 2003)
Hydroprocessing	$4.00/barrel produced
Natural gas (for backup)	$2.50/thousand standard cubic ft as the average wellhead price for 2007 (Peters 2003)
Ash/Char disposal	$23.87/tonne (Administration 2009)
Waste water disposal	$3.30/hundred cubic ft (Phillips 2007)
Electricity	$0.06/kWh
Sulfur	$44/tonne (Phillips 2007)
Fischer-Tropsch catalyst (cobalt)	$15/lb and 64 lb/ft^3 density; applied on first operation year and then every three years
Water-gas-shift catalyst (copper-zinc)	$8/lb and 900 kg/m^3; applied on first operation year and then every three years. Sour shift and normal WGS are assumed to operate with same catalyst.
Steam methane reforming catalyst (nickel-aluminum)	$15/lb and 70 lb/ft^3; applied on first operation year and then every three years.
Pressure swing adsorption packing	$2.1/lb

Fixed operating costs include employee salaries, overhead, and maintenance, and insurance and taxes. Salaries are calculated similarly to Phillips et al. (Phillips, Aden et al.

2007) where employees include a plant manager, shift supervisors, lab technician, maintenance technician, shift operators, yard workers, and office clerks. The labor index developed by the Bureau of Labor Statistics (Phillips, Aden et al. 2007) is used to adjust the labor cost to 2012$. Overhead is calculated as 60% of total salaries; maintenance cost and taxes/insurance cost are both 2% of total installed equipment cost as in accordance with Aden et al.(Statistics 2008)

For this analysis, the total capital investment is spent over a 2.5 year construction period, with 8% in the first half year, followed by 60% and 32% for the next two years. Working capital is applied in the year before operation and recovered at the end of the plant life. A standard modified accelerated cost recovery system (MACRS) is used, with the steam plant depreciating over 20 years and the rest of the plant over a 7 year period consistent with IRS allowances. The project life is 20 years. Plant availability of 310 days per year (85%) is assumed and affects raw materials purchase as well as fuel production. The PV per gallon of gasoline equivalent is calculated for a set net present value of zero including a 10% internal rate of return.

4.1 Methodology for Major Equipment Costs

The software used in the study is not capable of determining the price of each and every equipment used in the biorefinery. Special equipments like the gasifier and the Fischer – Tropsche reactor are special pieces of equipment that are underestimated if estimated as a simple vertical pressure vessel. Therefore, literature sources have been used to help estimate sizes and costs of many units. The following section details a few of the more important units.

The biomass dryer costs are estimated by determining the drying contact area. According to Couper (Aden, Ruth et al. 2002), typical rotary dryers have a diameter of 6 feet and solids holdup of 8%. Assuming a bulk density of 100 kg/m^3 for ground stover and 1000 kg/m^3 for moisture in the stover, the resulting total surface area required for drying is 1880 m^2. The surface area provides enough information for estimating the costs since rotary dryer costs are estimated based on surface area in Aspen Icarus.

With a similar kind of approach the lock-hopper is modeled using by referring to a Department of Energy report completed by Combustion Engineering, Inc. (Couper 2003) where residence times and operating pressures are given. The biomass receiving bin, lock hopper, and feed bin costs are then estimated with Aspen Process Economic Evaluator.

The fluidized bed gasifier installed cost is calculated according to equation 4.3, where $Cost_{0\_gasifier}$ is \$6.41 million (\$2003), $Stream\ Size_0$ is 41.7 metric ton per hour, and n is 0.7. The gasifier is evaluated at 300 short tons per day because that appears to be the highest proven capacity for GTI gasifier. It is assumed that the gasifier train follows the train cost formula (equation 4.2) resulting in \$19 million installed.

$$Cost_{gasifier} = Cost_{0\_gasifier} * \left[\frac{Stream\ Size}{Stream\ Size_0}\right]^n \qquad (4.3)$$

In a similar manner the FT reactor is estimated as described in Larson et al. where base installed cost is \$10.5 million (\$2003), base sizing value is 2.52 million standard cubic feet per hour of synthesis gas flow, and sizing exponent of 0.72. A installation factor of 3.6 is assumed for the FT reactor as found in Peters et al. (Larson, Jin et al. 2009) for liquid production plants. This allows the purchased cost of the unit to be back calculated.

Information from Phillips et al. (Peters, Timmerhaus et al. 2003) is used to calculate the price of the acid gas removal unit. The cost is found out using equation 4.3. The base stream size is 4000 short tons per day and base cost is $5.45 million. The stream size is the mass flow of the synthesis gas entering the AGR as the sum of fresh syngas from gas scrubbing and unconverted syngas from fuel synthesis area.

Capital investment for the hydroprocessing area is found in Robinson et al.(Phillips, Aden et al. 2007) That study reports a volumetric unit cost of $4,000 per barrel per standard day. Assuming the typical hydroprocessing refinery produces 25,000 barrels per day the base cost, C_0 is $100 million. Assuming a scaling exponent of 0.65, the cost of area 500 is found using equation 4.3.

CHAPTER 5. RESULTS AND DISCUSSION

5.1 Gasification Kinetics

Results of using the above two models described in the sections 3.2.1.2 and 3.2.1.3 are presented. First, a single operating condition is used to illustrate the advantages and disadvantages of each model in comparison with the experimental data. Then, the multistep kinetics model is further validated against experimental data for various feedstock and operating conditions before it is finally exercised against feedstock and operating conditions that are not available from experiments to test the predictiveness of the model.

The RCSTR model in Aspen Plus is used in this study for solving the reaction kinetics. RCSTR can model equilibrium reactions simultaneously with rate-based kinetic reactions. Perfect mixing in the reactor is assumed. It is also assumed that oxygen reacts with carbon in a shrinking core fashion and the layer of ash peels off as it is formed. The RCSTR model is used especially when there are solids participating in the reactions, as in this study. The model also allows multiple numbers of feeds which are mixed internally. In the model, it is assumed that biomass breaks down into its constituents after entering the reactor. Biomass mainly consists of C, H, N, O, and S. Carbon will partly constitute the gas phase, which takes part in devolatilization, and the remaining carbon comprises part of the solid phase and subsequently results in char. The amount of char formed can be found from the mass balance. The amount of volatile material can be specified from the biomass approximate analysis. It is assumed that char only contains carbon. So, the amount of carbon in the volatile portion can be calculated by deducting the total amount of carbon in char from the total carbon in biomass.

For comparison, the RYIELD model predicts final compositions by specifying the reaction yield of each component. This model is useful when the reaction stoichiometry and kinetics are unknown and the yield distribution data are available. On the other hand, the RCSTR model can consider the reaction kinetics and predict product distributions. This model is useful when the reaction kinetics is available and there are multiple feeds in the system.

5.1.1 Comparison of Models with Experimental Data

A comparison of the experimental and simulation results for both models using maple-oak feedstock operating at 21% oxygen (air) gasification conditions can be found in Fig. 5.1 and Fig. 5.2. Similar trends can be shown for each feedstock; therefore only one is included in this study. The significant results include:

- The baseline (mass balance approach) is able to predict as many species as are available from experimental data, allowing for more inclusive results, but limiting the applicability of this model since each feedstock and operating condition must use a new set of experimental data to improve accuracy. The simulation results are taken from literature. (Tiarks 2012)
- Inaccuracies in data collection are represented by incomplete mass balance across the gasifier in the baseline model as elements like H_2 are under predicted and N_2 is over predicted.
- The kinetics model is able to predict major syngas species to a better degree of accuracy than the baseline however, larger hydrocarbons and other minor species are not able to be predicted due to lack of detailed kinetics within the model.

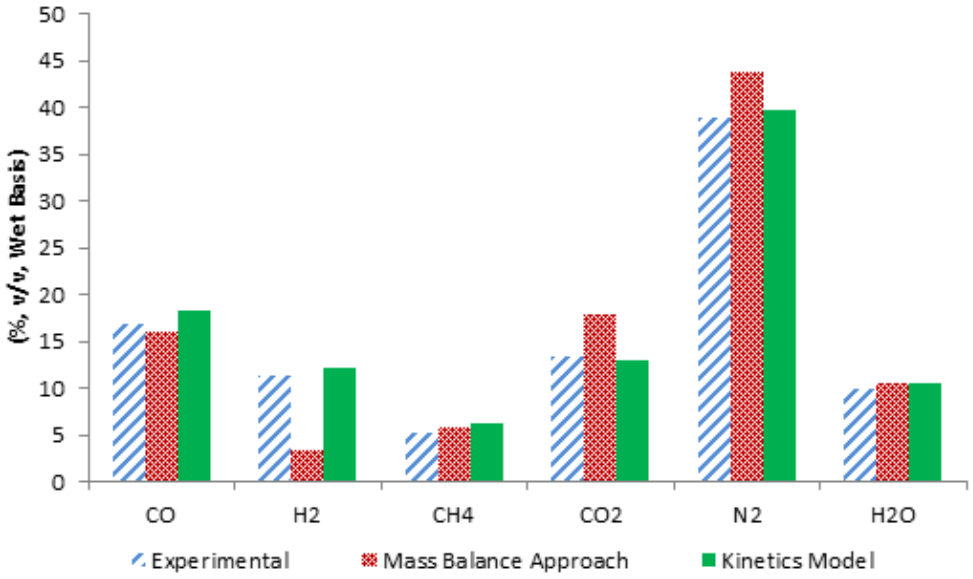

Fig. 5.1. Model comparison of main product gas compositions for maple-oak wood at 21% O_2

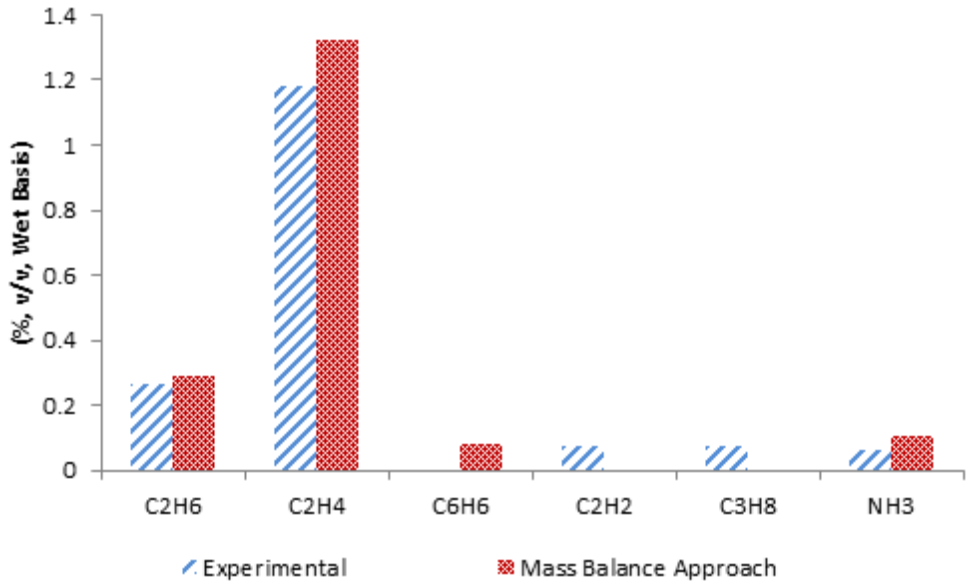

Fig. 5.2. Minor product gas compositions for maple-oak wood at 21% O_2 (kinetics model unable to predict)

5.1.2 Validation of Kinetics Model

The relationship between the major species concentration verses oxygen percentage used as a gasifying agent for various feedstocks is presented in Figures 5.3-5.5 for both the experimental data and kinetics model. Overall, the kinetics model is able to predict the major species for multiple feedstocks within several percent (v/v), and can be assumed fairly accurate across the feedstocks and operating parameters considered in this study.

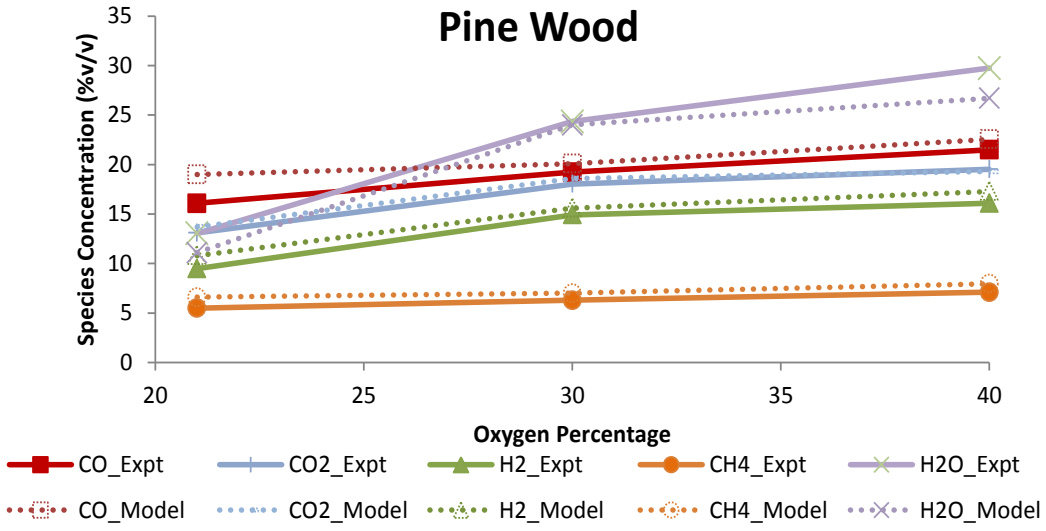

Fig. 5.3. Kinetics model validation of major syngas components for pine wood at various O_2%

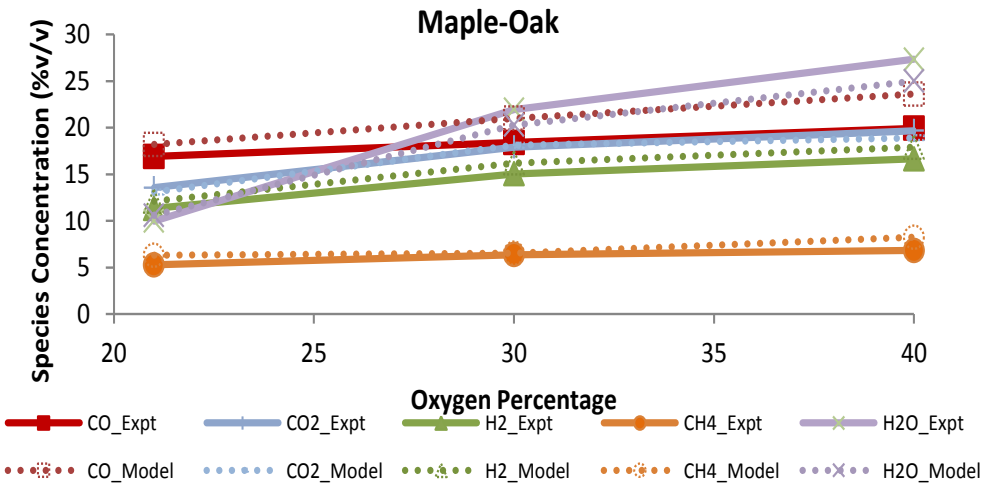

Fig. 5.4. Kinetics model validation of major syngas components for maple-oak wood at various O_2%

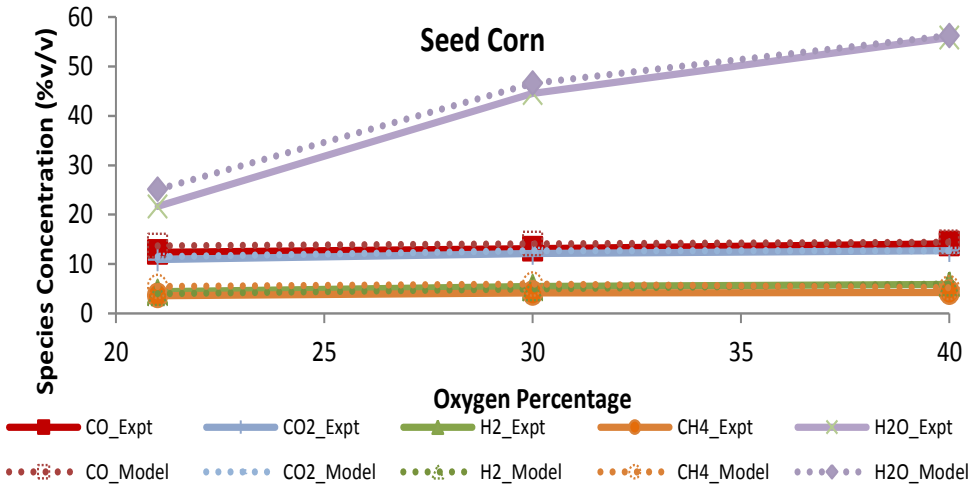

Fig. 5.5. Kinetics model validation of major syngas components for seed-corn at various O_2%

5.1.3 Effects of Oxygen and Steam

Steam is used to increase the reactivity of the system. With the use of air as the gasifying agent the heating values of the syngas produced is very low. When mixture of oxygen and steam are used, syngas with higher heating values (10-12 MJ/m^3) are formed.

With increase in oxygen concentration, the species concentration changes which are shown in Figures 5.6-5.9.

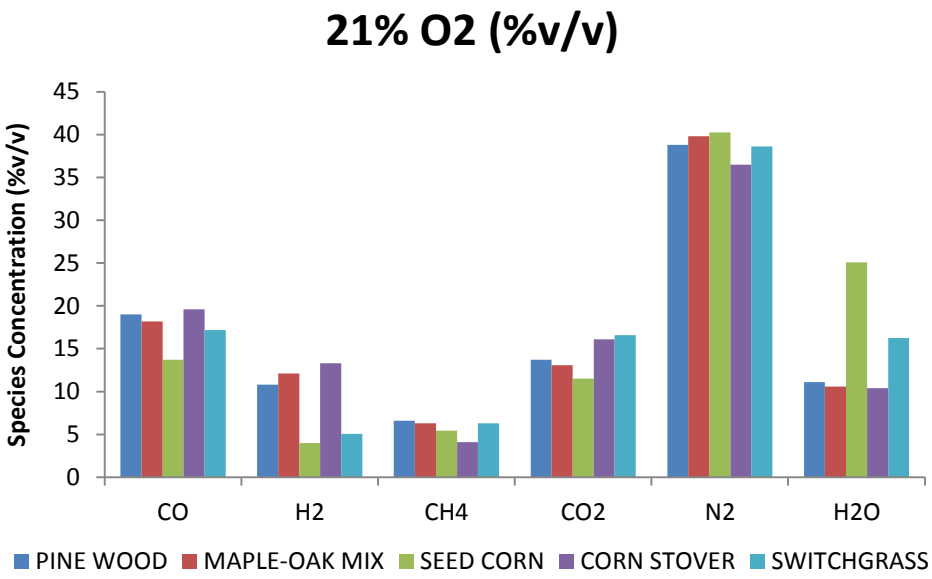

Fig. 5.6. Kinetics model comparison of various feedstock product gas compositions at 21% O_2

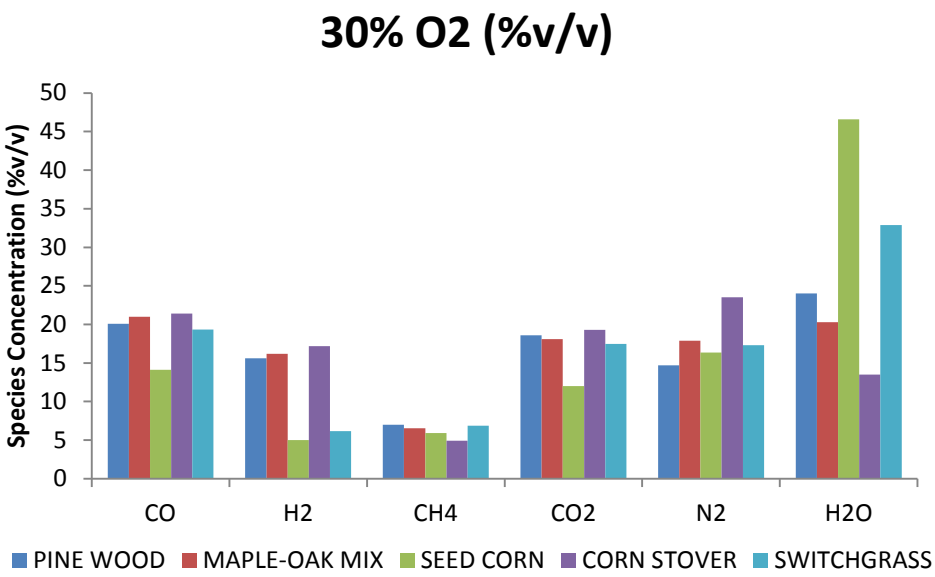

Fig. 5.7. Kinetics model comparison of various feedstock product gas compositions at 30% O_2

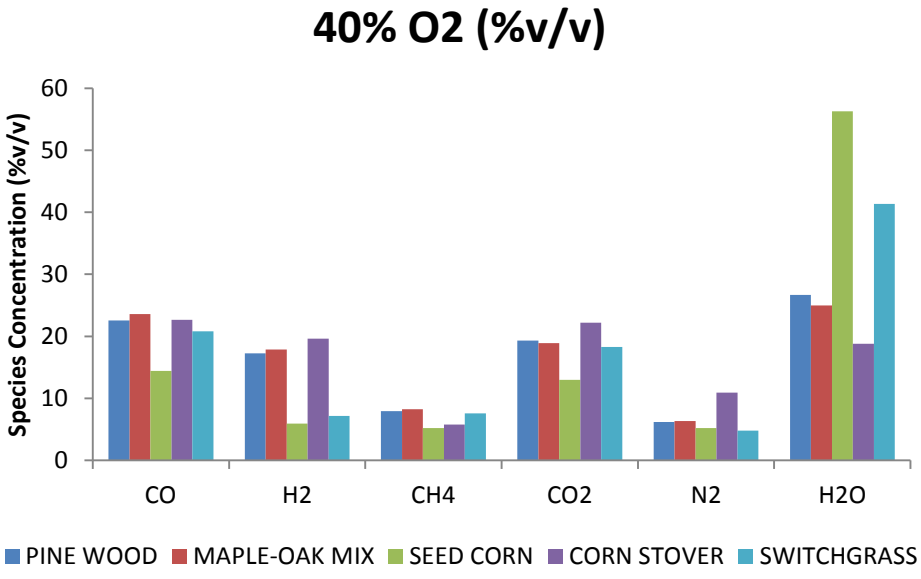

Fig. 5.8. Kinetics model comparison of various feedstock product gas compositions at 40% O_2

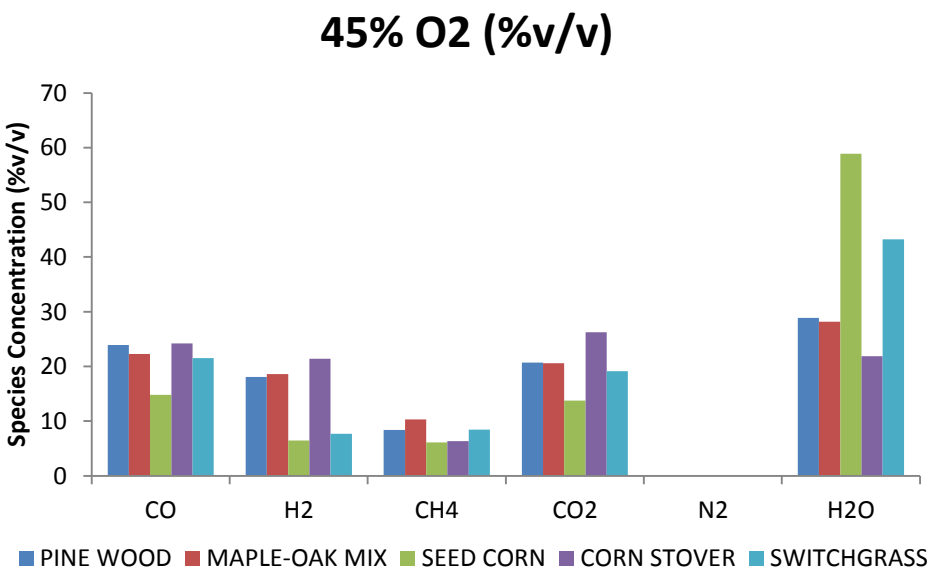

Fig. 5.9. Kinetics model comparison of various feedstock product gas compositions at 45% O_2

5.1.4 Effects of Different Feedstocks

The effects of different feedstocks on the syngas composition are shown in Figures 5.10-5.14. The results of the different effects are discussed in the next section.

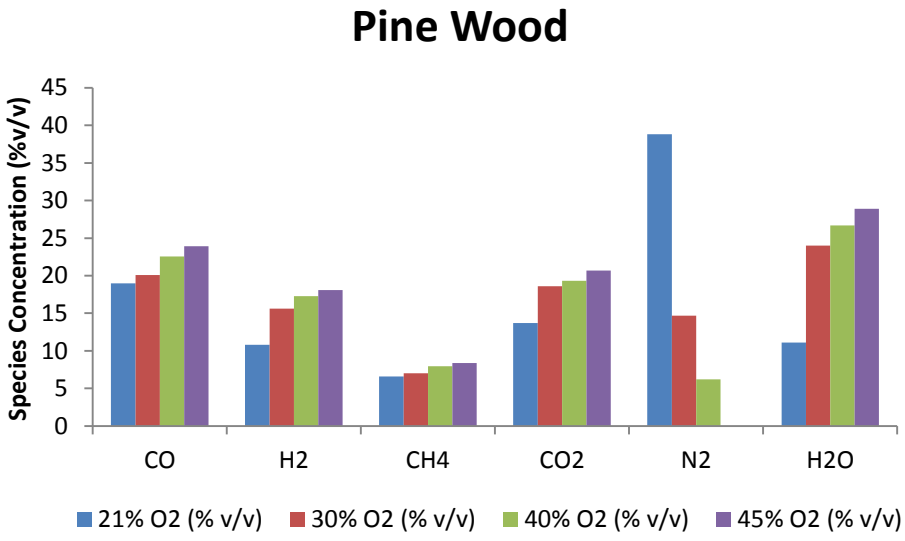

Fig. 5.10. Kinetics model main product gas compositions for pine wood at various O_2%

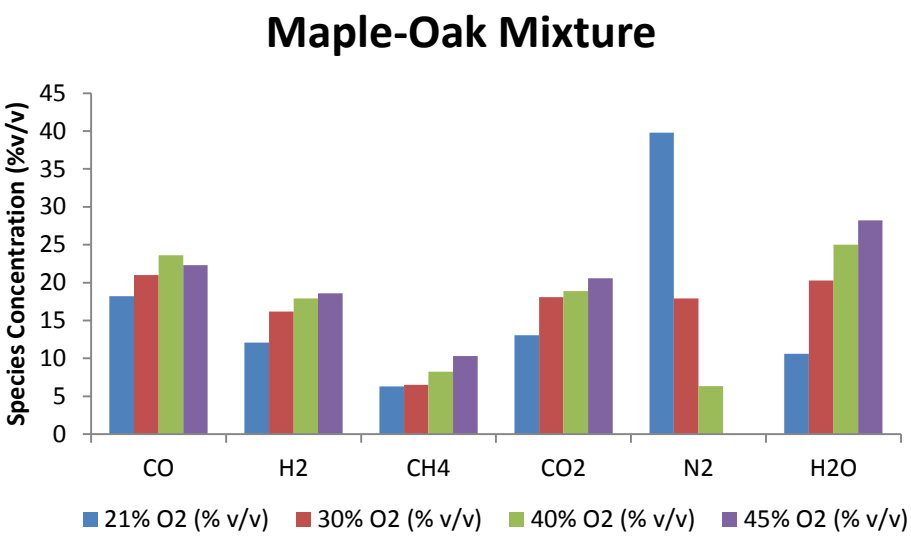

Fig. 5.11. Kinetics model main product gas compositions for maple-oak mixture at various O_2%

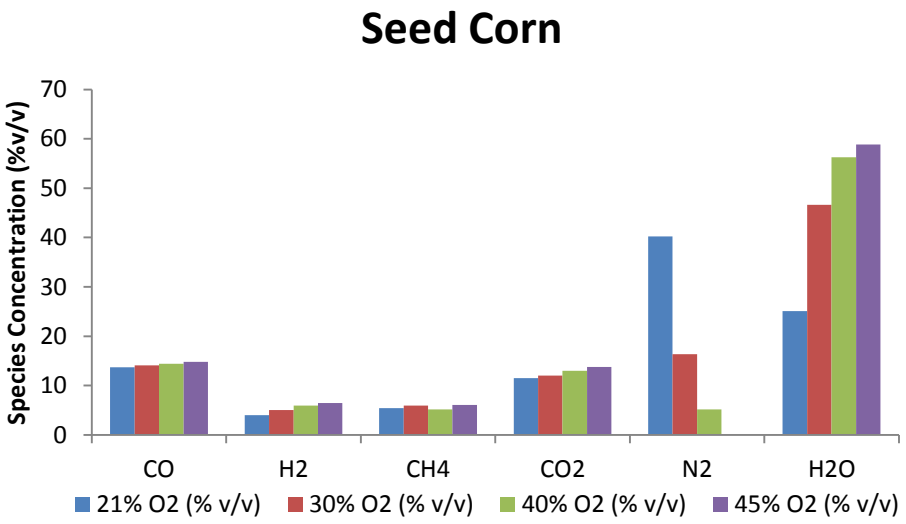

Fig. 5.12. Kinetics model main product gas compositions for seed corn at various O_2%

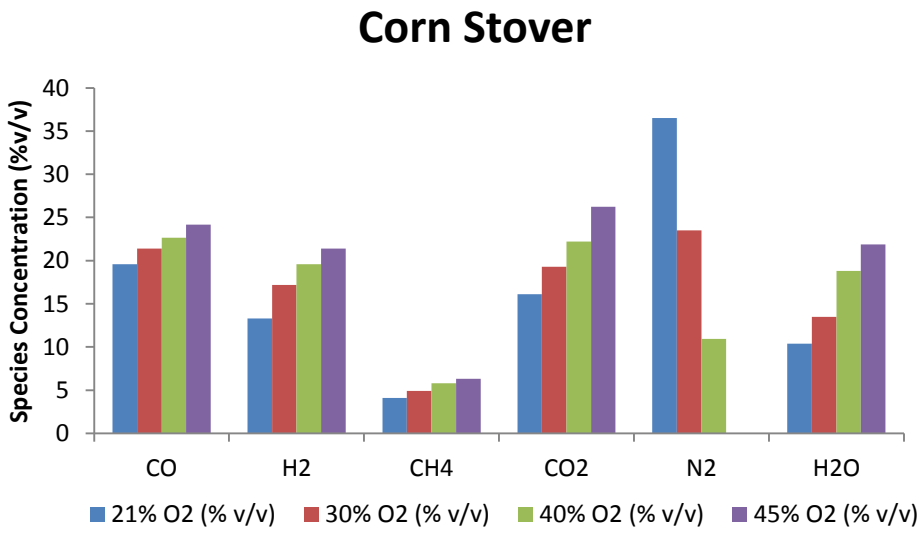

Fig. 5.13. Kinetics model main product gas compositions for corn stover at various O_2%

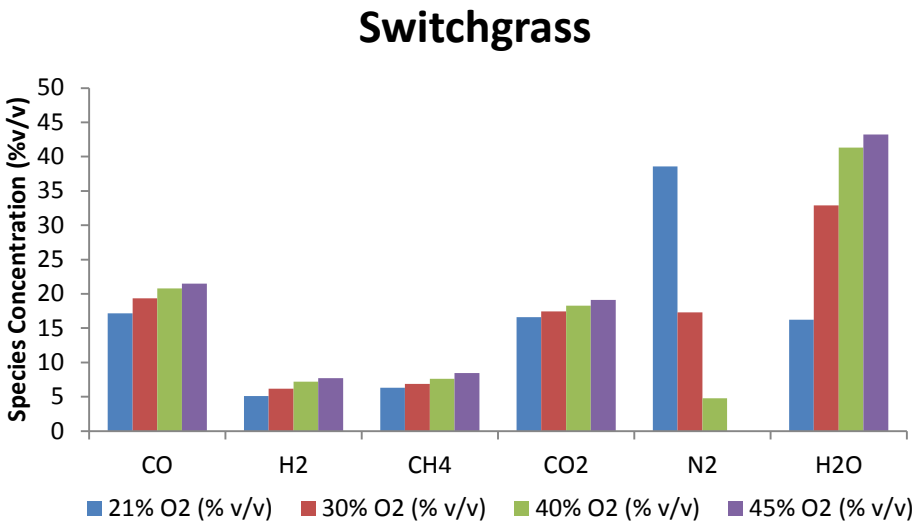

Fig. 5.14. Kinetics model main product gas compositions for switchgrass at various O_2%

5.1.5 Effects on H_2/CO Ratio

H_2 and CO are the most important gas components of syngas and can determine the syngas quality and downstream applications. For instance, to synthesize syngas into liquid fuels using Fischer-Tropsch processes, the optimal H_2/CO ratio is 2. In this study, although significant improvements in H_2 and CO are observed for all three feedstocks, the H_2/CO ratio is still below 2 under the current operating conditions. There is an increase in the H_2/CO ratio with increase in oxygen percentage from 21% TO 45%. The different H_2/CO ratio for different oxygen concentration is shown in Figure 5.15.

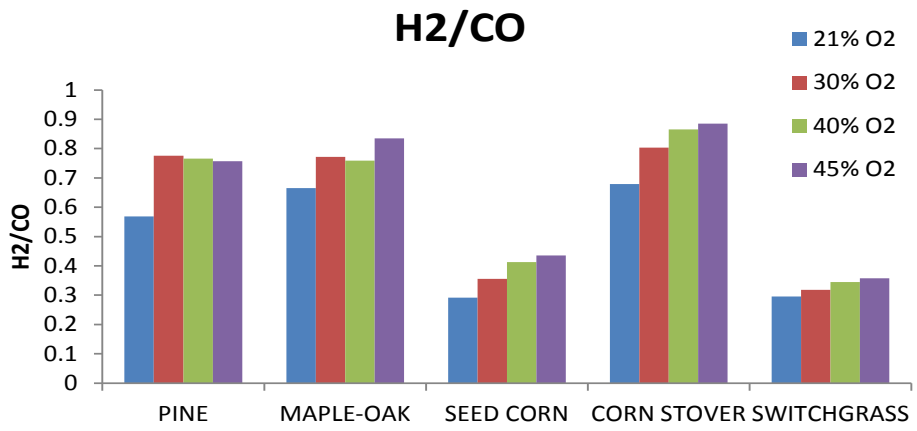

Fig. 5.15. H_2/CO ratio for different O_2%

5.1.6. Discussions

Due to similar trends in all the feedstocks, only one biomass is chosen for discussion. It is evident from the figures that the major constituents of syngas increase for all the biomass feedstocks with increase in oxygen concentration from 21% to 45%, one can see an increase in hydrogen by about 70%. This occurs with increase in temperature which increases the rate

of steam methane reaction and produces more hydrogen and carbon monoxide from methane and steam (Zhou, Chen et al. 2009). Also, the increase in hydrogen can be attributed to steam. Also, the increase in hydrogen can be attributed to steam. With the increase in S/O ratio for 30%, 40% and 45% oxygen, there is an increase in the amount of hydrogen present in the syngas. This supports the idea that steam is the major driving force behind the increase in hydrogen concentration. Increases in oxygen concentration in the gasifying agent give the necessary energy to initiate the reactions to produce hydrogen. With increase in oxygen, partial combustion of the syngas takes place, thereby, producing heat. The syngas composition strongly depends on the temperature at which gasification is occurring. Temperatures greater than 800 ^{o}C are usually favorable for gasification (Lv, Xiong et al. 2004). Also, from Table 3.4, one can see that the hydrogen content in corn stover is highest among all the feedstocks. However, the hydrogen in the syngas produced from seed corn is lowest. This is because the moisture content in seed corn is substantially higher than other feedstocks and much of the available energy is spent in the drying of the biomass, thus less energy is left for oxidation reactions to produce H_2 and CO. Also, the percentage of CO also increases with an increase in oxygen percentage from 21% to 45%. The percent increase in CO concentration is less than that of H_2 increase because in the steam methane reforming, three moles of H_2 are formed in comparison to one mole of CO. Water gas shift reaction also contributes to the increase in H_2 concentration. With the increase in the oxygen percentage in the gasifying medium, extra heat is available for the gasification reactions and thus the carbon conversion efficiency increases. When gasification reactions increase, there is a better chance of cracking down the carbon in chars and thus the carbon conversion efficiency increases.

Syngas composition and quality are largely dependent on the type of biomass feedstocks. Due to the difference in the proximate and ultimate analyses of various feedstocks the heating values and quality of syngas varies. Thus, the location of a biorefinery and the amount and kind of feedstock available at particular areas are of concern in assessing the profitability of such a biorefinery. In this particular study, five different kinds of biomass feedstocks are used in an attempt to cover the various feedstocks available in USA.

Another important conclusion that can be drawn is with increase in oxygen percentage in the gasifying agent, the CO_2 percentage in the syngas also increases. This happens due to the conversion of CO to CO_2 in presence of oxygen. Also, the steam increases the amount of H_2 at the expense of converting CO to CO_2. For all the different biomass feedstocks, there is a slight increase in light hydrocarbon (CH_4) due to methanation reaction where more CH_4 is formed due to reaction of H_2 with CO and CO_2.

Pure oxygen as a gasifying agent is an attractive choice but due to the high cost of pure oxygen, often oxygen-enriched air and steam are used as a gasifying agent. Heating value and composition of syngas are strongly dependent on the nature and amount of gasifying agent used. Mixtures of oxygen-enriched air and steam increase the heating value and quality of the syngas. Apart from substantial increase in the heating values of the syngas produced, use of oxygen-steam mixture also results in decreased tar production. Additionally, it provides the necessary heat to make gasification reaction autothermal. However, with increase in oxygen concentration in the gasifying agent, combustion becomes dominant instead of gasifaction. The flue gas that is produced due to combustion does not contribute to the heating value of the syngas (Basu 2010). When steam is used, the product gas contains more hydrogen per unit of carbon; thereby increasing the H/C ratio (Basu 2010). When air is

used, the nitrogen present in it dilutes the product gas. Thus use of oxygen-enriched air and steam increases the heating value of the product gas.

5.2 Biorefinery

5.2.1 Baseline Condition

In the baseline condition, purchased steam at 200 ^{o}C is used in the biorefinery for biomass drying, gasification and steam methane reforming. The biorefinery operates at 2000 tonnes/day of biomass.

5.2.1.1 Process Simulation Results

The total power usage in the biorefinery is 15 MW. Major contributions to this result are a lower grinder power due to less strict biomass size requirement, lower pressurized oxygen consumption in gasifier, and generally lower downstream mass flow rates throughout the plant for the particular scenario. The detailed power consumption for the biorefinery is given in Table 5.1. In addition to the production of transportation fuels, electrical power is generated from the non-condensable gases from the gasification section, part of the flue gas from the combustion section, and part of unconverted syngas. The total power generated is 31 MW. In total, 16 MW of electricity is produced and sold as a byproduct. Thus, the biorefinery is self-sustained and the excess power produced is sold adding to the profitability of the plant. The net power usage in the plant can be reduced depending on the optimization of the stream flow rates, recycle ratios, conversion efficiencies, heat integration within the biorefinery. The scope of this study is to produce liquid fuels from biomass. Procedures to optimize recycle ratios, equipment sizes, and fuel production rates are not within the scope of this study and are not undertaken.

Table 5.1. Power genration and usage of each section

	Plant Area	**Power (MW)**
Usage	Chopper (A100)	0.50
	Grinder (A100)	1.10
	Lock hopper system (A200)	0.20
	Lean Amine Solution Pump(A300)	0.7
	Syngas Booster Compressor (A300)	1.0
	PSA Compressor (A400)	0.1
	Recycle Compressor (A400)	0.3
	Hydroprocessing Area (A500)	1.75
	Oxygen compressor (ASU) (A700)	2.80
	Air Compressor (ASU) (A700)	6.3
	CO_2 Compressor	0.4
	Total Usage	**15.14**
Generation	Gas Turbine	21.0
	Steam Turbine	10.40
	Total Generated	**31.4**
Net Export		**16.3**

Based on energy balance, the overall energy efficiency to convert biomass to fuel is 39% on a LHV basis. When the net electricity is added, the conversion efficiency is 43% on LHV basis. The detailed analysis is given in Table 5.2. The scenario is expected to be lower since mass and energy loss occurs in the production and removal of char and tar. Char and tar

energy loss sums to 7.5% of the energy in the biomass. A significant amount of chemical energy is contained in tar and biochar. Biochar from the gasification section is directed to the combustion chamber and the resulting hot flue gas provides part of the heat required to reheat the steam for drying biomass. The most significant loss is in the gasifier. About 25% energy is lost in the gasifier. One reason for high energy loss is because thermodynamic efficiency increases with increasing operating temperature. More effective capture of the energy in the hot syngas would increase the overall energy efficiency.

Table 5.2. Overall energy balance on LHV basis

	Fraction
IN	
Biomass	1.000
OUT	
Fuel	-0.39
Net Electricity	-0.043
Power Gen Losses	-0.030
FT reactor losses	-0.125
Gasifier losses	-0.250
Char	-0.064
Tar	-0.013
Syngas Purge	0.000
Total	-0.915

A carbon balance analysis shows that 26 percent of the carbon in the biomass is converted to the fuels for the scenario. The detailed analysis of the carbon balance is given in Table 5.3. Approximately 99% carbon is being accounted for. The major loss in carbon is

carbon dioxide flue gases, LO-CAT venting and lock hopper venting. Char leaving the scenario is accounted for in the flue gas since the char is combusted for process heat. The biorefinery produces low molecular weight hydrocarbons in the gasification process, a small fraction become dissolved in the liquid effluent of the wet scrubber. Carbon dioxide also dissolves in wet scrubber effluent stream. Another carbon loss comes from the hydrocarbons that dissolve in the acid gas removal area.

Table 5.3. Overall carbon balance

	Fraction
IN	
Biomass	1.000
OUT	
Fuel	0.265
A300 CO2 Vent	0.395
A600 Flue Gas	0.090
A200 Flue Gas	0.070
Lock hopper Vent	0.050
Wet Scrubber Effluent	0.098
Tar	0.010
Dissolved Hydrocarbons	0.015
Total	0.993

Steam and cooling water are required as utilities in various processes in the biorefinery. A pinch analysis (a method to optimize heat exchange) is not included in this particular study. So, the integration of heat streams is not optimized in this study.

5.2.1.2 Capital and Operating Costs for the Plant

The total capital investment for the baseline case is approximately $561 million. The cost breakdown and the resulting total capital investment are shown in Tables 5.4 and 5.5 respectively. The installation cost is shown in Fig. 5.16 for each plant area. The fuel synthesis section, power generation unit, syngas cleanup zone, and the gasification section account for the major investment. A breakdown of the major cost categories is shown in Fig. 5.17. Using a DCFROR analysis, the PV at a net present value of zero for the baseline case is $5.14/GGE. (GGE is Gallons of Gasoline Equivalent)

The major area of investment in the scenario is the fuel synthesis section. Steam methane reformer and heat exchange equipments are required for the higher operational temperature. A significant portion of the capital cost is due to gas compression such as the air compressor in the air separation unit and syngas booster compressor. Due to high purchase costs, compressors make up approximately 18% of the TPEC for each scenario.

Table 5.4 Results from the baseline biorefinery

Parameter	**Value**
Plant Size (tonne/day)	2,000
Total Capital Investment ($MM)	561
Availability (hour/year)	7,446
Rate of Return (%)	10
Fuel Yield (MMGGE/yr)	32.3
Product Value ($/GGE)	**5.14**

Table 5.5. Capital investment breakdown for the n^{th} plant scenario

Plant Area	**Results**	
	($MM)	% of TIC
Preprocessing	25.1	8
Gasification	31.8	11
Syngas Cleaning	33	12
Fuel Synthesis	66.1	23
Hydroprocessing	33.3	12
Power Generation	43.9	15
Air Separation Unit	21.9	8
Balance of Plant	30.7	11
Total Installed Cost (TIC)	**285.5**	
Indirect Cost (IC)	**120.62**	
Total Direct and Indirect Cost (TDIC=TIC+IC)	**406.5**	
Contingency (20% of TDIC)	**81.3**	
Fixed Capital Investment (FCI=TDIC+Contingency)	**487.8**	
Working Capital (15% of FCI)	**73.2**	
Total Capital Investment (TCI=FCI+Working Capital)	**560.9**	

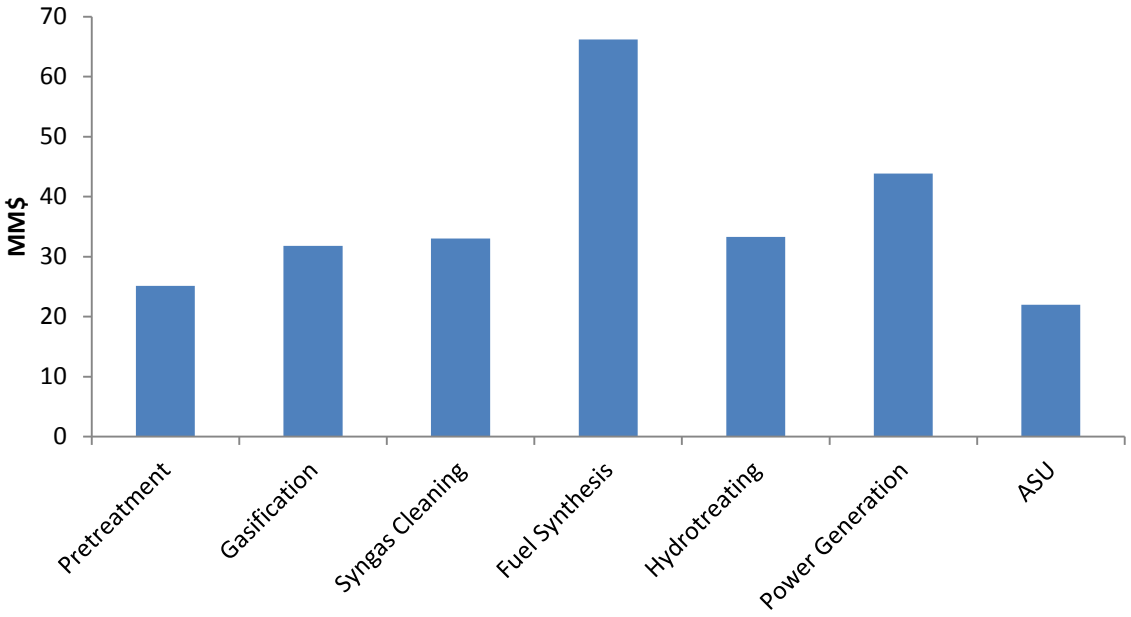

Figure 5.16. Total installation costs of the biorefinery according to plant areas

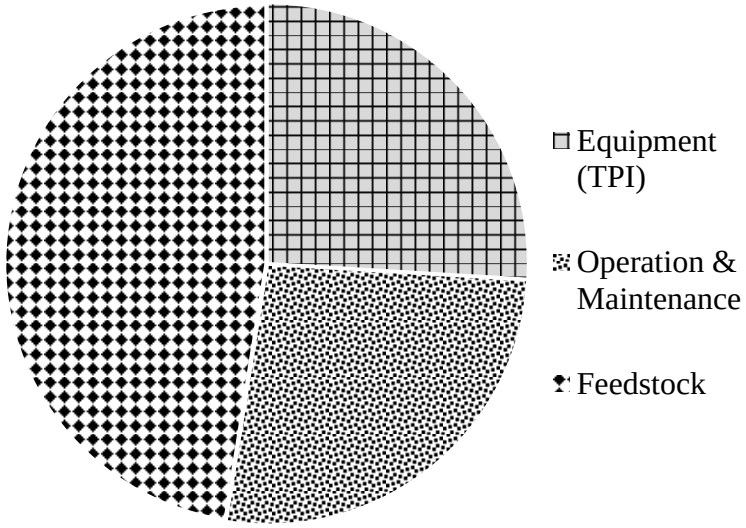

Figure 5.17. Cost breakdown of the biorefinery based on 20 years of operation

Annualized costs for operation of the plant are shown in Table 5.6. The percentage displayed also represents percentage of product value (PV). The largest annual incurred costs for both scenarios are the average return on investment and feedstock purchase. Utilities such as steam and cooling water are high in the scenario due to heating and cooling of the syngas before and after the steam methane reformer (SMR) and steam input to the SMR. The catalyst costs are not determined on an annual basis since they are assumed to be replaced every three years. The catalysts costs are given in Table 5.7.

Table 5.6. Annual operating cost breakdown for n^{th} plant scenario

	Annual operating costs
Average Return on Investment	$48,300,000
Feedstock	$51,300,000
Capital Depreciation	$21,900,000
Average Income Tax	$18,200,000
Fixed Costs	$12,500,000
Hydroprocessing	$3,000,000
Steam	$3,500,000
Cooling Water	$3,500,000
Waste Disposal	$1,500,000
Other Raw Matl. Costs	$1,400,000
Co-product credits	-$7,320,000

Table 5.7. Catalyst replacement costs (3 year replacement period)

Catalyst	Price
Water-gas-shift (copper-zinc)	$106,800
Steam reforming (nickel-aluminum)	$105,600
ZnO guard bed	$435,400
PSA packing	$499,500
Fischer-Tropsch (cobalt)	$6,150,800

5.2.2 Study 1: Using Geothermal Steam for Gasification and Reforming

In this case study, geothermal-derived steam (further called "geothermal steam") is used to replace the purchased steam for gasification and steam reforming. Geothermal steam is produced when the geothermal liquid, extracted from production wells at a flowrate of 105 kg/s and 180°C, passes through a heat exchanger to produce geothermal steam. The temperature of the geothermal steam is 150 ^{o} C with a flow rate of 16 kg/s (i.e., 1,382 tonne/day) supplying steam throughout the biorefinery. As a gasifying agent, 352 tonne/day of steam is required and 1,000 tonne/day is necessary for steam-methane reforming at the present plant capacity. Steam upgrading occurs between the hot flue gas and geothermal steam in a downstream heat exchanger in order to achieve the required temperatures for use as a gasifying and steam-methane reforming agent. Results are obtained assuming that the price of the produced 150°C geothermal steam is $12/MMBtu (Anderson 2012). A schematic of the geothermal resource distribution is shown in Fig. 5.18. It should be noted that an

additional stream of geothermal liquid is supplied to the Organic Rankine Cycle as discussed in the next section.

Based on the above cost of geothermal steam, economic study shows that the price of fuel is $5.42/GGE (Table 5.8), which is comparable to the baseline case. In the original setup, approximately 100 tonne/day of natural gas is needed to produce the required steam. By using geothermal steam, this natural gas is no longer needed, thus reducing fossil fuel consumption and greenhouse gas emissions significantly. As a result, integrating geothermal energy into the biorefinery is economically feasible and more environmentally sustainable.

A sensitivity study on the price of geothermal energy is conducted as shown in Table 5.9 . It can be seen that the cost of the product fuel is moderately sensitive to the cost of geothermal steam. This is mainly because the price of steam only constitutes a small percentage of the total operating cost. Therefore, it can be concluded that the use of geothermal energy in a biorefinery is viable.

Table 5.8. Biorefinery product value using geothermal energy for gasification and fuel reforming

Parameter	**Value**
Plant Size (tonne/day)	2,000
Fuel Yield (MMGGE/yr)	32.4
Product Value ($/GGE)	**5.42**

Table 5.9. Sensitivity analysis by varying geothermal steam price

	Cost of geothermal heat ($/MMBtu)	Cost of gasoline ($/GGE)
Baseline	n/a	$5.14
	$0	$5.02
	$10	$5.36
Average	$12	$5.42
	$15	$5.51
	$20	$5.66

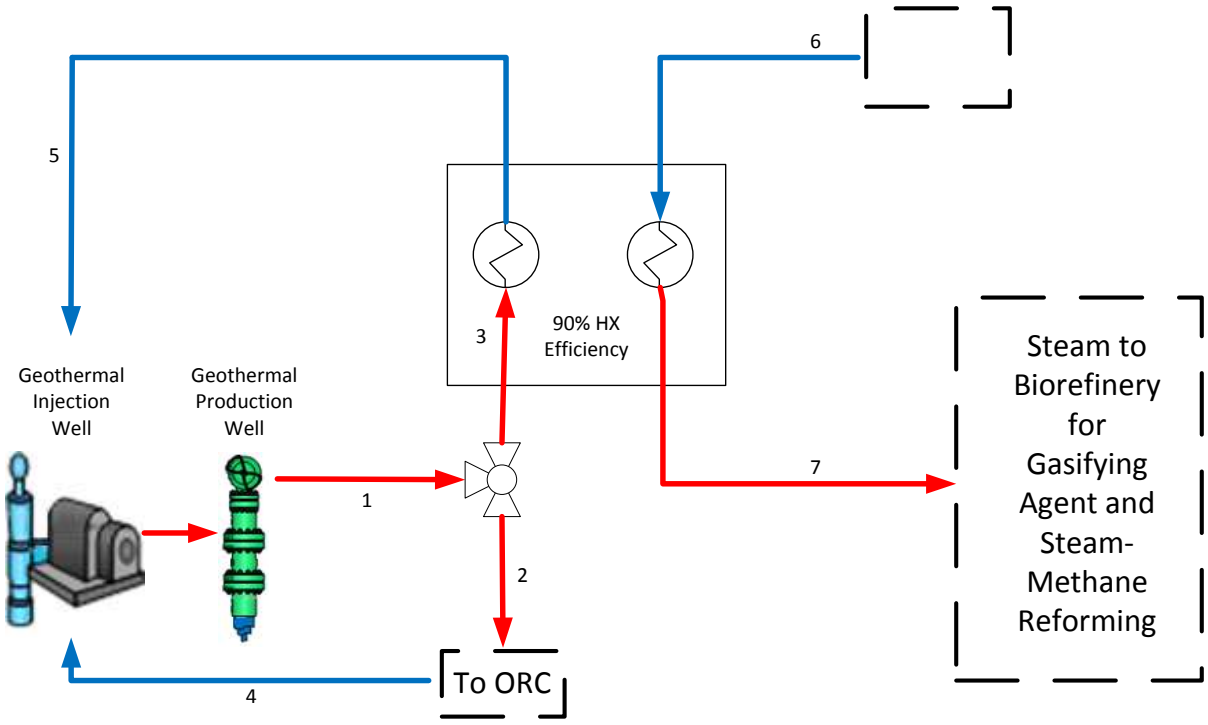

State	Temperature	Pressure	Enthalpy	Mass Flow Rate	Method of Calculation
	°C	bar	kJ/kg	kg/s	
1	180	10	761.39	205	$\dot{m}_1 = \dot{m}_3 + \dot{m}_4$
2	180	10	741.39	100	Avg. flow of 2 wells
3	180	10	761.39	105	$\dot{m}_3 = \frac{\dot{m}_6(h_7 - h_6)}{0.9(h_3 - h_4)}$
4	75	10	314.8	100	$\dot{m}_4 = \dot{m}_2$
5	75	10	314.8	105	$\dot{m}_5 = \dot{m}_3$
6	25	1.01	104.89	16	Aspen Model
7	150	4	2752	16	Aspen Model

Figure 5.18. Schematic of the geothermal resource distribution to the biorefinery and corresponding stream properties

5.2.3 Study 2: Using Geothemal Steam for Power Generation via ORC

The total amount of geothermal steam required for gasification and steam-methane reforming is 1,352 tonne/day based on the present biorefinery plant capacity. This geothermal steam requirement corresponds to roughly a requirement of 9072 tonne/day geothermal liquid supply, corresponding to approximately two geothermal wells for this flowrate. Additionally, it is possible that multiple wells can be drilled at the same site due to the advancement of the drilling technology. Thus, there remains excess geothermal steam for other potential use.

A suitable way to utilize the excess geothermal energy is to produce electricity via the Organic Rankine Cycle (ORC), which is a proven technology to produce electricity from low-grade energy sources. ORC uses an organic, high molecular weight fluid with a low boiling point to allow the Rankine cycle to recover energy from geothermal heat. The working fluid in ORC plays a key role as it determines the performance and the economics of the plant. The characteristics and favorable working fluids can be found in literature (Anderson 2012). The energy and exergy analyses based on the first and second laws of thermodynamics are evaluated in this study for the organic working fluid under diverse working conditions. For simplicity, the internal irreversibility and the pressure drops in evaporators, condensers and pipes are neglected. Steady-state assumptions are used for analysis.

In this study, a stand-alone ORC model using R134a is first built using Aspen Plus, as shown in Fig. 5.19.

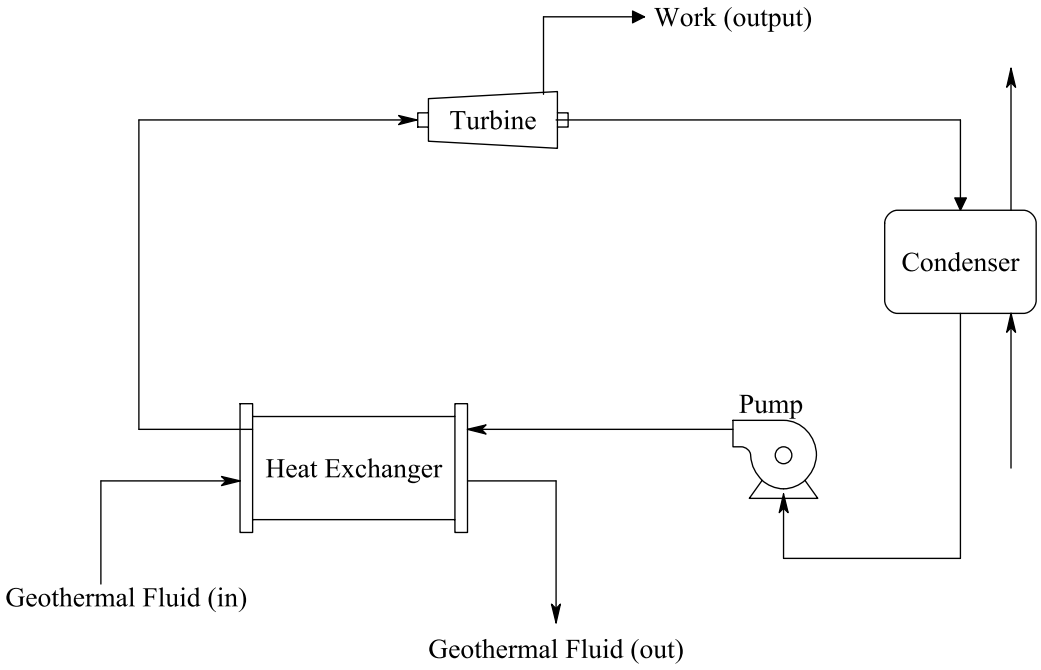

Figure 5.19. Flow diagram of the Organic Rankine Cycle

A preliminary parametric study is first conducted to investigate the effects of various operating parameters on the thermal efficiency and help determine the baseline operating conditions. The different operating parameters include the mass flow rate of the organic fluid ($\dot{m}_{R134a}$), temperature of the geothermal fluid ($T_{geo,in}$), pump inlet pressure (P_1), and turbine inlet pressure (P_2), as listed in Table 5.10.

Table 5.10. Range of ORC operating parameters

Parameter	**Range**
Geothermal source inlet temperature ($T_{geo,in}$)	100 – 200 ºC
Pump inlet pressure (P_1)	5 – 20 bar
Turbine inlet pressure (P_2)	20 – 70 bar
Mass flow rate of the organic fluid ($\dot{m}_{R134a}$)	100 – 300 kg/s

The following assumptions for the ORC model are made. (1) The isentropic efficiency of the turbine is 90% and no moisture is present in the exhaust. (2) The quality in the turbine exhaust is kept above 90% to reduce the risk of blade erosion. (3) The pump efficiency is 90%.

The utilization efficiency for ORC is defined as

$$\eta_u = \frac{W_{net}}{\dot{m} \cdot e} \qquad \text{eqn. (1)}$$

where $\dot{m}$ is the mass flow rate of geothermal fluid, W_{net} the net power output, and e the specific exergy, $e = h_1 - h_0 - T_0 (s_1 - s_0)$. Here, h_1 is the enthalpy of geothermal liquid at the inlet, h_0 is the enthalpy of geothermal liquid at the ambient condition, T_0 is the ambient temperature, s_1 is the entropy of geothermal liquid at the inlet, and s_0 is the entropy of geothermal liquid at the ambient conditions.

The parametric study is conducted in an iterative manner due to the inter-dependence of the parameters. Based on the results of the parametric study, baseline conditions for the ORC are determined as listed in Table 5.11.

Table 5.11. Operating parameters of ORC in the biorefinery

Parameter	**Value**
Geothermal source inlet temperature ($T_{geo,in}$)	180 °C
Pump inlet pressure (P_1)	10 bar
Turbine inlet pressure (P_2)	50 bar
Mass flow rate of the organic fluid ($\dot{m}_{R134a}$)	150 kg/s
Mass flow rate of geothermal fluid	100 kg/s

The geothermal liquid flow rate (100 kg/s) for ORC, together with the required quantity for biorefinery operation, is approximately equal to the capacity of four wells. According to the present parametric study, although a higher amount of geothermal liquid can increase the power production, it will require a large amount organic fluid and/or cause unreasonable operating conditions for the pump and turbine. As a result, the present ORC plant produces 4.5 MW of power with a utilization efficiency of 43%.

The efficiency of ORC also depends on the ambient temperature and geothermal liquid temperature, representing the local climate and geothermal conditions, respectively. Thus, a sensitivity study is further conducted. Fig. 5.20 shows that the utilization efficiency decreases with the ambient temperature. On the other hand, the thermal efficiency is defined as

$$\eta_t = \frac{W_{net}}{Q_{in}} \qquad \text{eqn. (2)}$$

where W_{net} is the net power output and Q_{in} is the net heat input into the system. The baseline thermal efficiency is 13% and the variation of thermal efficiency with respect to the inlet geothermal temperature is shown in Fig. 5.21.

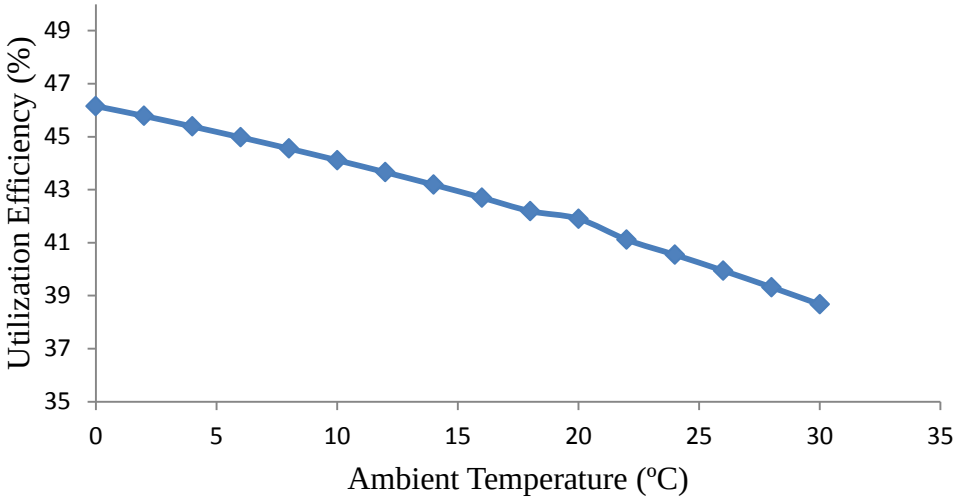

Figure 5.20. Utilization efficiency of ORC with respect to ambient temperature based on geothermal liquid inlet temperature at 180 ºC.

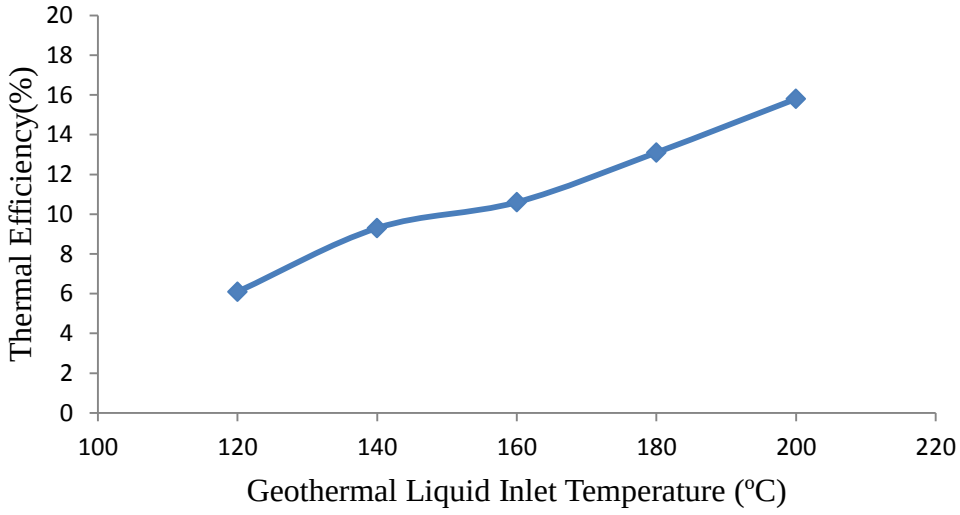

Figure 5.21. Thermal efficiency of ORC at various inlet temperature of geothermal steam

The above stand-alone ORC model is incorporated into the biorefinery model for integrated technical and economic analysis. Excess unused heat from the biorefinery is utilized in the ORC for additional power generation. The excess power generated is then sold to enhance th e profitability of the biorefinery. Costs associated with the ORC plant (e.g., installation, equipment, operation) are also considered in calculating the final fuel price. A sensitivity study is also conducted by varying the price of the geothermal liquid, as shown in Table 5.12. Results show that the fuel price is slightly reduced by incorporating the ORC plant.

Table 5.12. Fuel price based on the integrated biorefinery with ORC

Cost of Geothermal Energy ($/MMBtu)	**Product Value ($/GGE)**
10	5.18
12	5.24
15	5.34
20	5.50

Overall, the cost of fuels produced utilizing geothermal energy ($5.24/GGE) is comparable to the baseline conditions ($5.14/GGE). The major motivation to integrate geothermal energy into the biorefinery is the reduction in greenhouse gas emissions resulting from burning fossil fuels to generate the process steam. With the advancement in the drilling technology, the production cost of geothermal energy can be reduced in the future and thus the use of geothermal energy can become more feasible. This can be further enhanced by appropriate government policies to encourage the use of renewable energy and the reduction of greenhouse gas emissions.

CHAPTER 6. CONCLUSIONS

An Aspen Plus model is used to study the feasibility of transportation fuel production from corn stover via thermochemical processes. The technoeconomic analysis of the biorefinery is conducted to determine the minimum selling price of fuels produced. A number of methods are devised to utilize geothermal energy in the biorefinery. It is found that geothermal energy can potentially be used in a biorefinery for various purposes. In this study, geothermal heat is used to generate steam which in turn replaces the purchased steam for gasification and steam-methane reforming. The resulting fuel price utilizing geothermal energy is slightly higher, but still comparable to that of the baseline conditions. Excess, unused geothermal energy can also be used in an Organic Rankine Cycle to generate electricity to add profits to the biorefinery. Overall, the cost of fuels produced by utilizing geothermal energy ranges from $5.18 to $5.50 per gallon gasoline equivalent compared to $5.14 of the baseline condition. The above costs are based on the 2012 cost year. The major motivation to integrate geothermal energy into a gasification-based biorefinery appears to be the reduction in greenhouse gas emissions resulting from steam production using fossil fuels. The advancement in the drilling technology together with appropriate government incentives can further enhance the feasibility of utilizing geothermal energy for biofuel production.

In this study, a chemical kinetics model is also developed and validated to predict the syngas composition under various operating conditions. The oxygen percentage is increased from 21% to 45% (v/v). Five different kinds of feedstocks are used in the study for kinetics model validation—pine wood, maple-oak mixture (50/50), seed corn, corn stover, and switchgrass. The bed temperature is maintained at 800 ^{o}C. Different conditions including the flow rate of biomass and different oxygen and steam ratios are used for validation. The

simulation results of major syngas species are in good agreement with the experimental data for pine wood, maple-oak mixture, seed corn, and corn stover. The model is able to predict the effects of feedstock and oxygen-steam ratios. It can be seen that with increased oxygen percentage, the nitrogen dilution effect greatly decreases, thereby, increasing the heating values of the syngas. The use of steam can increase the production of H_2 and CH_4 for all the feedstocks. Thus, oxygen-enriched air with steam is a plausible option for gasification; however, the H_2/CO ratio is low and not very suitable for the Fischer-Tropsch process to produce liquid fuels from syngas. The ratio is low because much of the steam remains unreacted and shows up in the syngas stream. Thus, it is important to operate the gasifier at a much higher temperature than 800 ^oC because water-gas shift reaction works better and the effective conversion of steam to H_2 and CH_4 takes place at higher temperatures. More rigorous simulation has to be carried out to model NO_x, NH_3, and other higher alkane and alkenes species such as C_2H_4, C_2H_2, and C_2H_6, to predict gasification performance more accurately.

BIBLIOGRAPHY

Aden, A., Ruth, M., Ibsen, K., Jechura, J., Neeves, K., Sheehan, J., Wallace, B., Montague, L., Slayton, A., Lukas, J. (2002). Lignocellulosic Biomass to Ethanol Process Design and Economics Utilizing Co-current Dilute Acid Prehydrolysis and Enzymatic Hydrolysis for Corn Stover. Golden, Colorado, USA.

Administration, E. I. (2009, 2/25/2009). "U.S. Natural Gas Wellhead Price." Retrieved March 1 2009, 2009, from http://tonto.eia.doe.gov/dnav/ng/hist/n9190us3m.htm.

Amos, W. A. (2008). Report on Biomass Drying; NREL/TP-570-25885, National Renewable Energy Laboratory, Golden, Colorado, USA.

Anderson, B. (2012). Private communication. Stanford University, Palo Alto, CA.

Bain, R. L. (1992). Material and Energy Balances for Methanol from Biomass Using Biomass Gasifiers, National Renewable Energy Laboratory.

Banerjee, S., Tiarks, J., Zhang, Y., Kong, S.-C., Meyer, T.-R., Brown, R.-C., Anderson, B. (2011). Techno-Economic Analysis of Biorefinery Utilizing Geothermal Energy For Processing. Paper SGP-TR-194. Proceedings of the Thirty-Seventh Workshop on Geothermal Reservoir Engineering. Stanford University, San Fransisco, California, USA.

Barbier, E. (2002). "Geothermal energy technology and current status: an overview." Renewable & Sustainable Energy Reviews 6: 1: 3-65.

Basu, P. (2010). Biomass Gasification and Pyrolysis: Practical Design and Theory. Elsevier.

Bridgwater, A. V. (1995). "The Technical and Economic-Feasibility of Biomass Gasification for Power-Generation." Fuel 74: 5: 631-653.

Bridgwater, A. V., Toft, A. J., Brammer, J. G. (2002). "A techno-economic comparison of power production by biomass fast pyrolysis with gasification and combustion." Renewable & Sustainable Energy Reviews 6: 3: 181-246.

Brown, R. C. (2003). Biorenewable resources: engineering new products from agriculture. Ames, IA, Iowa State Press.

Caputo, A. C., Palumbo, M., Pelagagge, P.-M., Scacchia, F. (2005). "Economics of biomass energy utilization in combustion and gasification plants: effects of logistic variables." Biomass & Bioenergy 28: 1: 35-51.

Chen, G., Andries, J., Spliethoff, H., Fang, M. (2004). "Biomass gasification integrated with pyrolysis in a circulating fluidised bed." Solar Energy 76: 1-3: 345-349.

Chen, H. J., Goswami, D. Y., Stefanakos, E. K. (2010). "A review of thermodynamic cycles and working fluids for the conversion of low-grade heat." Renewable & Sustainable Energy Reviews 14: 9: 3059-3067.

Couper, J. R. (2003). Process engineering economics. New York, Marcel Dekker.

Damartzis, T., Zabaniotou, A. (2011). "Thermochemical conversion of biomass to second generation biofuels through integrated process design-A review." Renewable & Sustainable Energy Reviews 15: 1: 366-378.

DiPippo, R. (2012). Geothermal Power Plants: Principles, Applications, Case Studies and Environmental Impact, Elsevier.

E. I. A. (2011). Annual Energy Outlook 2011 with Projections to 2035.

E. P. A. (2010). "Regulation of Fuels and Fuel Additives: Changes to Renewable Fuel Standard Program." Rules and Regulations 75 (58).

Gil, J., Aznar, M. P., Caballero, M. A.; Frances, E., Corella, J. (1997). "Biomass gasification in fluidized bed at pilot scale with steam-oxygen mixtures. Product distribution for very different operating conditions." Energy & Fuels 11: 6: 1109-1118.

Giltrap, D. L., McKibbin, R., Barnes, G. R. G. (2003). "A steady state model of gas-char reactions in a downdraft biomass gasifier." Solar Energy 74: 1: 85-91.

Huber, G. W., Iborra, S., Corma, A. (2006). "Synthesis of transportation fuels from biomass: Chemistry, catalysts, and engineering." Chemical Reviews 106: 9: 4044-4098.

Hung, T. C., Shai, T. Y., Wang, S. K. (1997). "A review of organic Rankine cycles (ORCs) for the recovery of low-grade waste heat." Energy 22: 7: 661-667.

Huynh, C. V., Kong, S. C. (2012). "Combustion and NOx Emissions of Biomass-Derived Syngas under Various Gasification Conditions Utilizing Oxygen-Enriched-Air and Steam." Fuel (in press).

Huynh, C. V., Kong, S. C. (2012). "Performance Characteristics of a Pilot-Scale Biomass Gasifier Using Oxygen-Enriched Air and Steam." Fuel (in press).

Imperial Chemical Industries, l. A. D. (1970). Catalyst handbook: with special reference to unit processes in ammonia and hydrogen manufacture. London, UK.

Inc., Nexant. (2006). Equipment Design and Cost Estimation for Small Modular Biomass Systems, Synthesis Gas Cleanup, and Oxygen Separation Equipment. N. Inc., National Renewable Energy Laboratory, Golden, Colorado, USA.

Kaushal, P., Abedi, J., Mahinpey, N. (2010). "A comprehensive mathematical model for biomass gasification in a bubbling fluidized bed reactor." Fuel 89: 12: 3650-3661.

Kohl, A. L., Nelson, R. B. (1997). Gas Purification. Houston, Gulf Professional Publishing.

Larson, E. D., Jin, H., Celik, F. E. (2009). "Large-scale gasification-based coproduction of fuels and electricity from switchgrass." Biofuels, Bioproducts, and Biorefining 3: 2: 174-194.

Larson, E. D., Jin, H., Calik, F. E. (2005.). Gasification-Based Fuels and Electricity Production from Biomass, without and with Carbon Capture and Storage. Biofuels.

Lau, F. S., D. A. Bowen, Dihu, R., Doong, S., Hughes, E. H., Remick, R., Slimane, R., Turn, S. Q., Zabransky, R. (2002). Techno-Economic Analysis of Hydrogen Production by Gasification of Biomass, Gas Technology Institute.

Lv, P., Yuan, Z. H., Ma, L. L., Wu, C. Z., Chen, Y., Zhu, J. X. (2007). "Hydrogen-rich gas production from biomass air and oxygen/steam gasification in a downdraft gasifier." Renewable Energy 32: 13: 2173-2185.

Lv, P. M., Xiong, Z. H., Chang, J., Wu, C. Z., Chen, Y., Zhu, J. X. (2004). "An experimental study on biomass air-steam gasification in a fluidized bed." Bioresource Technology 95: 1: 95-101.

Maizza, V., Maizza, A. (2001). "Unconventional working fluids in organic Rankine-cycles for waste energy recovery systems." Applied Thermal Engineering 21: 3: 381-390.

Mani, S., Tabil, L. G., Sokhansanj, S. (2004). "Grinding performance and physical properties of wheat and barley straws, corn stover and switchgrass." Biomass & Bioenergy 27(4): 339-352.

Mathieu, P., Dubuisson, R. (2002). "Performance analysis of a biomass gasifier." Energy Conversion and Management 43(9â€“12): 1291-1299.

Nikoo, M. B. and N. Mahinpey (2008). "Simulation of biomass gasification in fluidized bed reactor using ASPEN PLUS." Biomass & Bioenergy 32: 12: 1245-1254.

Patwardhan, P. R., Brown, R. C., Shanks, B. H. (2011). "Understanding the Fast Pyrolysis of Lignin." Chemsuschem 4: 11: 1629-1636.

Peters, M. S., Timmerhaus, K. D., West, R. E. (2003). Plant design and economics for chemical engineers. New York, McGraw-Hill.

Phillips, S., Aden, A., Jechura, J., Dayton, D., Eggemen, T. (2007). Thermochemical Ethanol via Indirect Gasification and Mixed Alcohol Synthesis of Lignocellulosic Biomass, National Renewable Energy Laboratory, Golden, Colorado, USA.

Pollard, A. S., Rover, A. S., Brown, R. C. (2012). "Characterization of bio-oil recovered as stage fractions with unique chemical and physical properties." Journal of Analytical and Applied Pyrolysis 93: 129-138.

Reed, M. E., Van Bibber, L., Shuster, E., Haslbeck, J., Rutkowski, M., Olsen, S., Kramer, S. (2007). Baseline Technical and Economic Assessment of a Commercial Scale Fischer-Tropsch Liquids Facility, National Energy Technology Laboratory, USA.

Roy, P. C., Datta, A., Chakraborty, N. (2009). "Modelling of a downdraft biomass gasifier with finite rate kinetics in the reduction zone." International Journal of Energy Research 33: 9: 833-851.

Sethuraman, S., Huynh, C. V., Kong, S. C. (2011). "Producer Gas Composition and NOx Emissions from a Pilot-Scale Biomass Gasification and Combustion System Using Feedstock with Controlled Nitrogen Content." Energy & Fuels 25: 813-822.

Sharma, A. K. (2008). "Equilibrium and kinetic modeling of char reduction reactions in a downdraft biomass gasifier: A comparison." Solar Energy 82: 10: 918-928.

Spath, P. L., Dayton, D. (2003). Preliminary Screening -- Technical and Economic Assessment of Synthesis Gas to Fuels and Chemicals with Emphasis on the Potential for Biomass-Derived Syngas.

Swanson, R. M., Platon, A., Satrio, J. A., Brown, R. C. (2010). "Techno-economic analysis of biomass-to-liquids production based on gasification." Fuel 89: S2-S10.

Sudiro, M., Zanella, Bressan, L., Fontana, M., Bertucco, A. (2009). Synthetic natural gas (SNG) from petcoke: model development and simulation. Proceedings of the 9th International Conference on Chemical and Process Engineering (ICheaP-9).

Tester, J. W., Drake, E. M., Driscoll, M. J., Golay, M.W., Peters, W.A. (2005). Sustainable Energy: Choosing Among Options, MIT Press, Cambridge, MA.

Tian, F.-J., Jianglong, Y., McKenzie, Lachlan J., Hayashi, J., Li, Chun-Zhu. (2007). "Conversion of Fuel-N into HCN and NH during the Pyrolysis and Gasification in Steam: A Comparative Study of Coal and Biomass." Energy & Fuels 21: 517-522.

Tiarks, Jordan A. (2012). “Investigation of biomass gasification and effects of ammonia on producer gas combustion.” Mechanical Engineering, Iowa State University, Ames, IA, USA.

Tijmensen, M. J. A., Faaij, A. P. C., Hamelinck, C. N., van Hardeveld, M. R. M. (2002). "Exploration of the possibilities for production of Fischer Tropsch liquids and power via biomass gasification." Biomass and Bioenergy 23: 2: 129-152.

Wali, E. (1980). "Working Fluids for Solar, Rankine-Cycle Cooling Systems." Energy 5: 7: 631-639.

Wang, Y., Kinoshita, C. M. (1993). "A Kinetic-Model of Biomass Gasification." Energy from Biomass and Wastes 10: 6: 841-855.

Warnecke, R. (2000). "Gasification of biomass: comparison of fixed bed and fluidized bed gasifier." Biomass and Bioenergy 18: 6: 489-497

Yan, H. M., Rudolph, V. (2000). "Modelling a compartmented fluidised bed coal gasifier process using aspen plus." Chemical Engineering Communications 183: 1-38.

Yoshioka, T., Hirata, S., Matsumura, Y., Sakanishi, K. (2005). "Woody biomass resources and conversion in Japan: The current situation and projections to 2010 and 2050." Biomass & Bioenergy 29: 5: 336-346.

Zhou, J. S., Chen, Q., Zhao, H., Cao, X.W., Mei, Q. F., Luo, Z. Y., Cen, K. F. (2009). "Biomass-oxygen gasification in a high-temperature entrained-flow gasifier." Biotechnology Advances 27: 5: 606-611.